Quantum Spintronics Design
(NV centers in diamond)

Eisuke Abe

RIKEN Center for Quantum Computing

2022.9.7

CMD Spintronics Design Course

(Online)

Diamond envy

III (13)	IV (14)	V (15)
B	C	N

©GIA

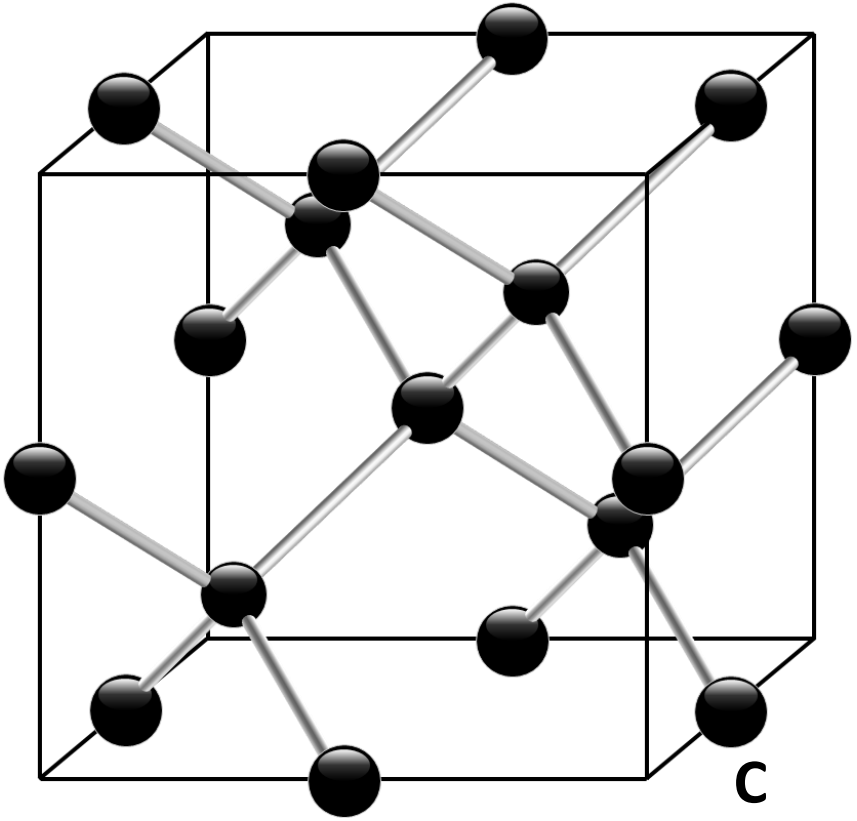

$\rho_N = 1.77 \times 10^{23}\ cm^{-3}$

Diamond envy

III (13)	IV (14)	V (15)
B	C	N

©GIA

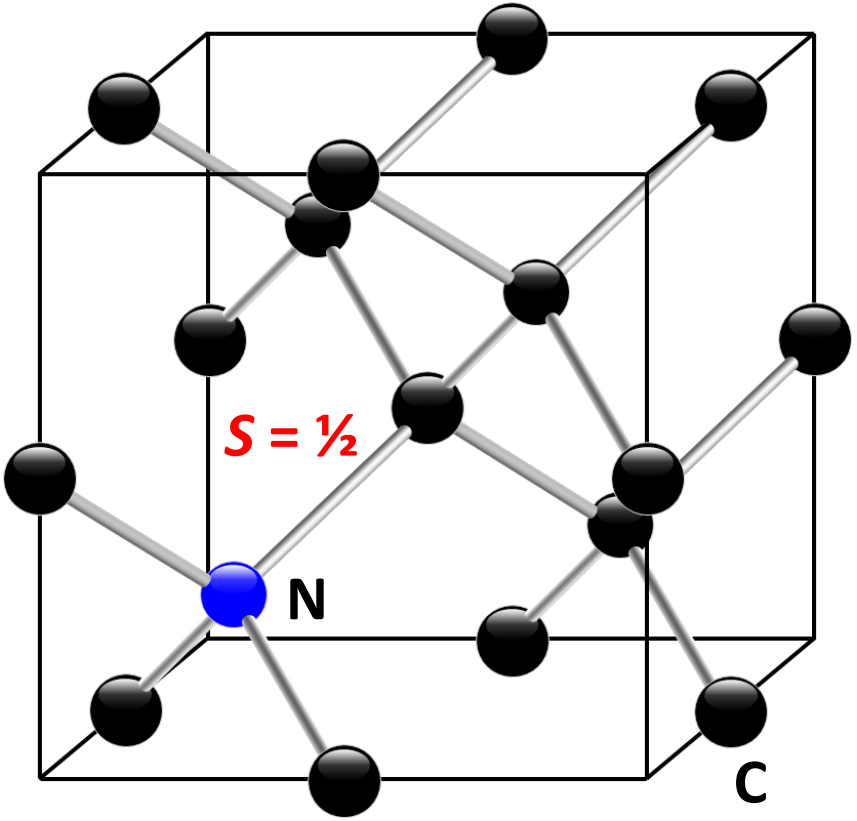

$\rho_N = 1.77 \times 10^{23}\ cm^{-3}$

Diamond NV

III (13)	IV (14)	V (15)
B	C	N

©GIA

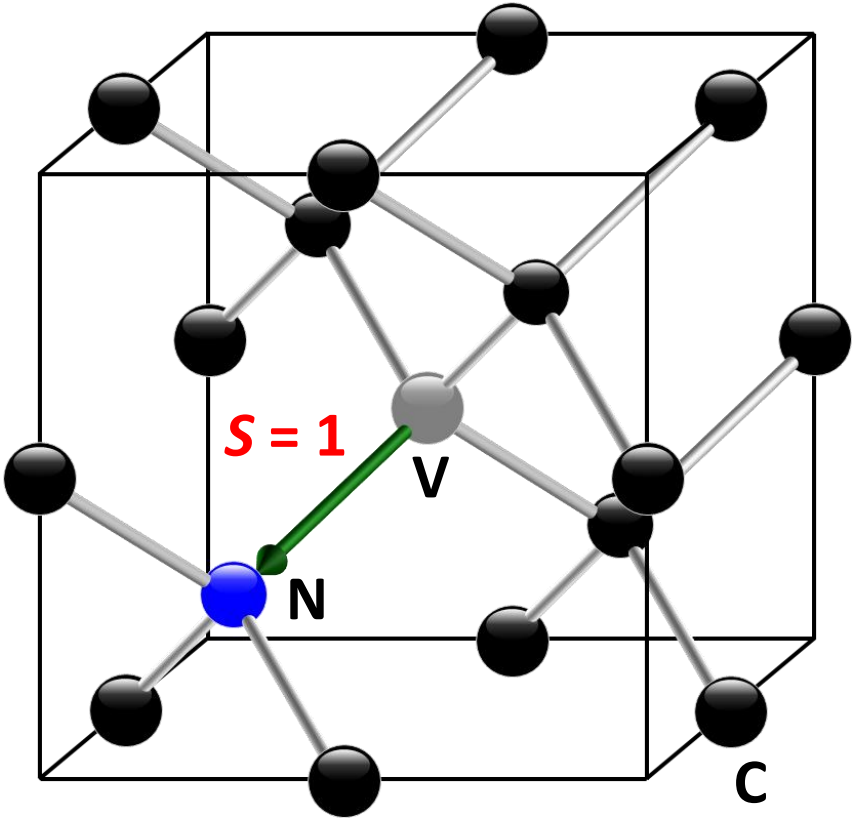

$\rho_N = 1.77 \times 10^{23}\ cm^{-3}$

Diamond NV

Synthetic (CVD) diamond
2 x 2 x 0.5 mm^3, $700 (E6)
[N] < 5 ppb, [NV] < 0.03 ppb

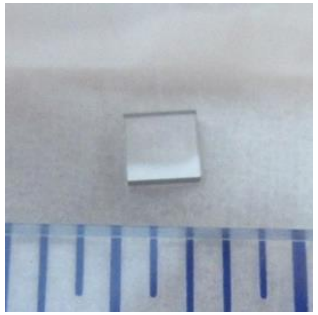

Not like…

©GIA

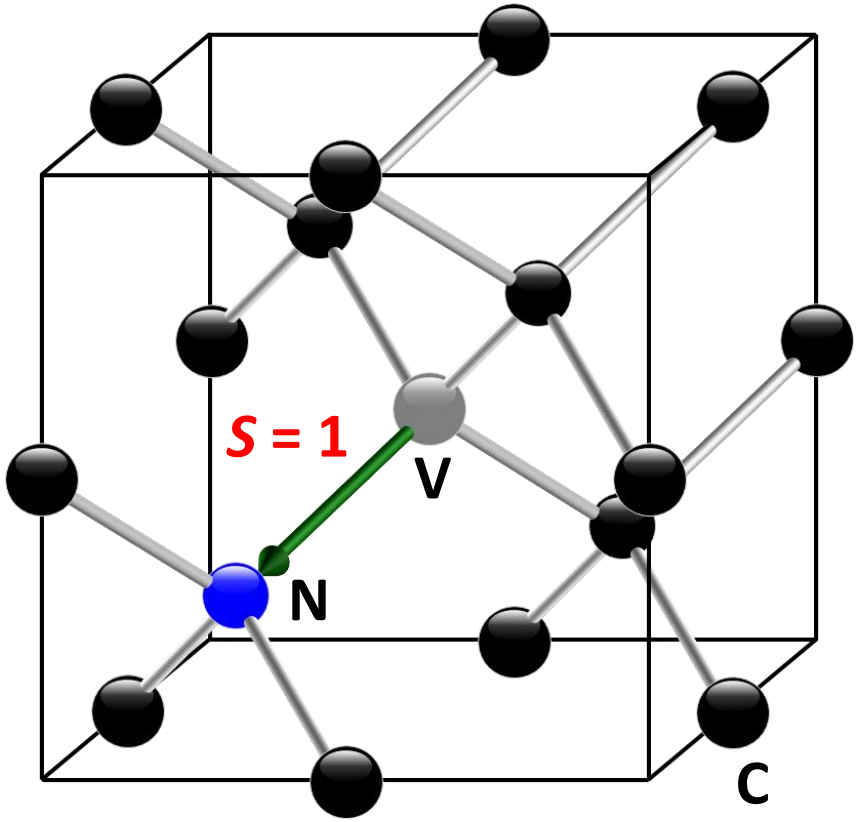

$\rho_N = 1.77 \times 10^{23}\ cm^{-3}$

Diamond NV

Synthetic (CVD) diamond
2 x 2 x 0.5 mm^3, $700 (E6)
[N] < 5 ppb, [NV] < 0.03 ppb

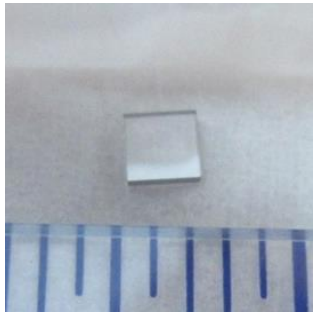

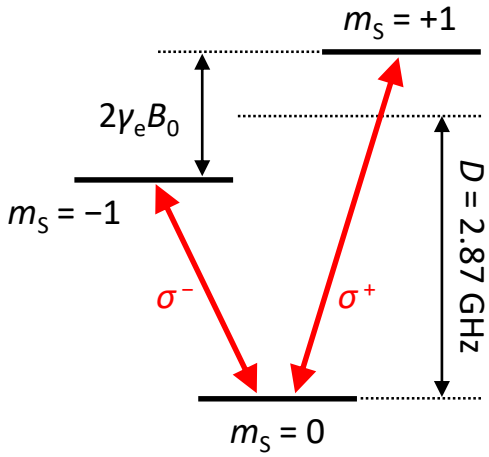

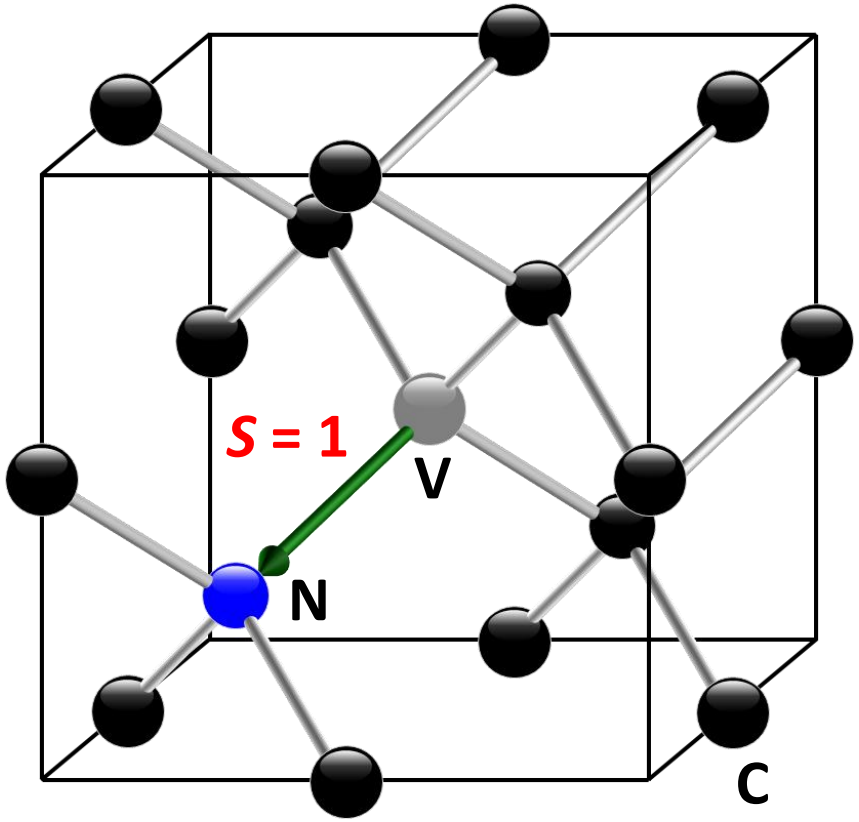

$\rho_N = 1.77 \times 10^{23}$ cm^{-3}

Quick overview

- Optical detection & initialization of single spins
- Microwave control of single spins
- Room temperature operation

PL mapping

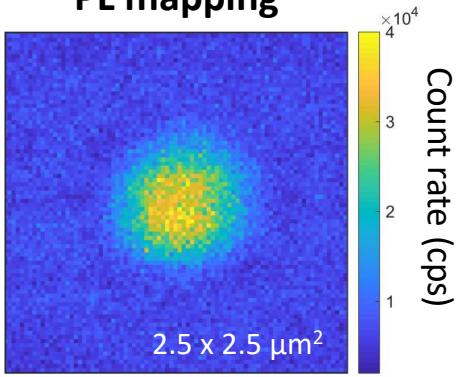

Optically detected magnetic resonance (ODMR)

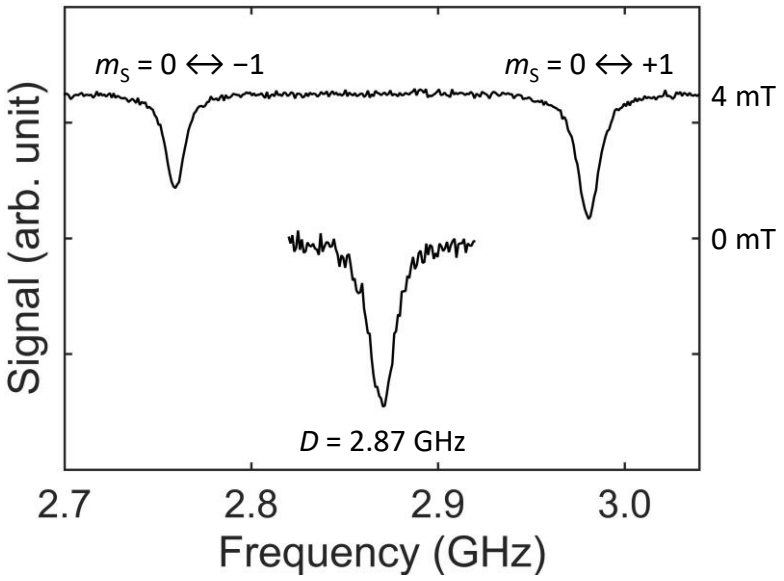

Rabi oscillation

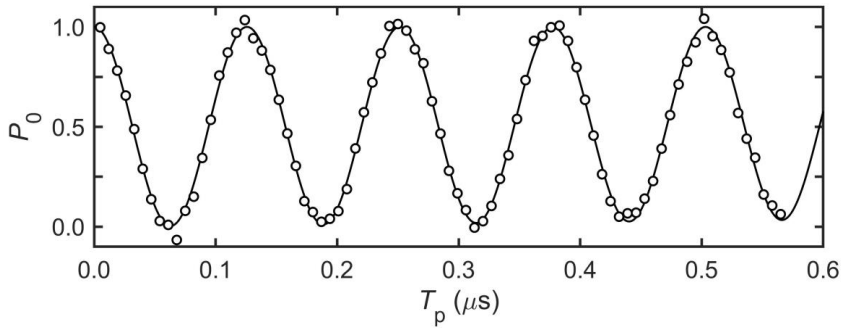

Quantum sensing with NV centers

- *B*, *E*, *T*, *S*…
- DC & AC modes
- Wide temperature range
- Nondestructive
- High spatial resolution
- Various modalities

Nanodiamond & biology

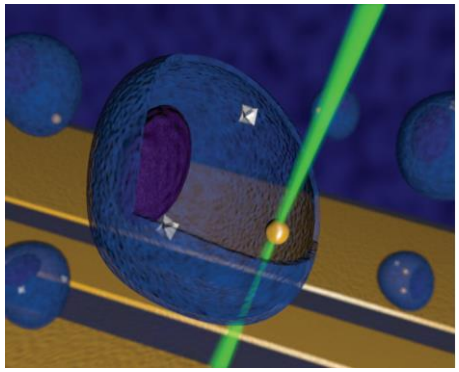

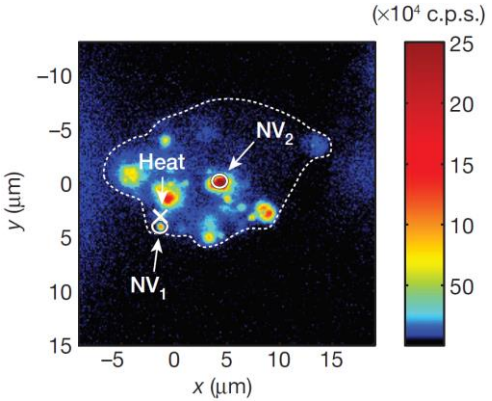

Nature **500**, 54 (2013)

Near-surface NV center & NMR

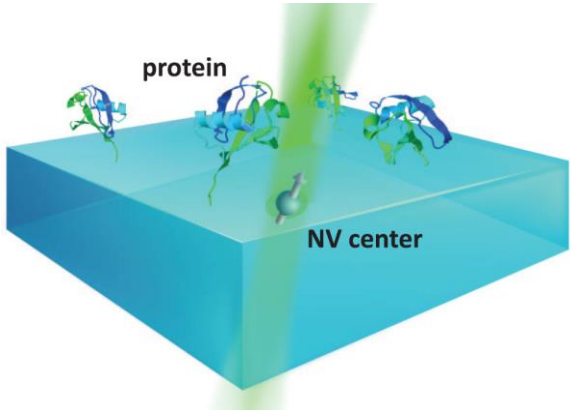

Science **351**, 836 (2016)

Scanning probe & condensed matter

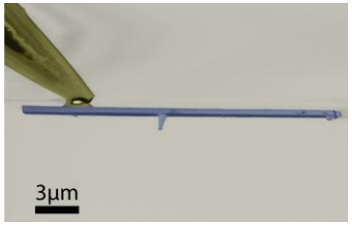

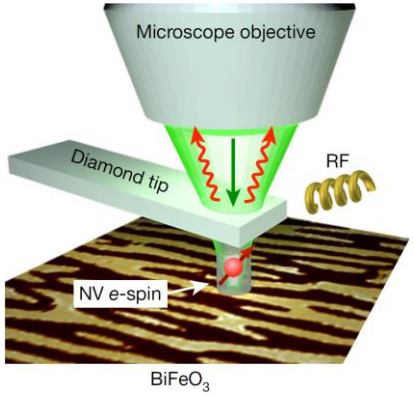

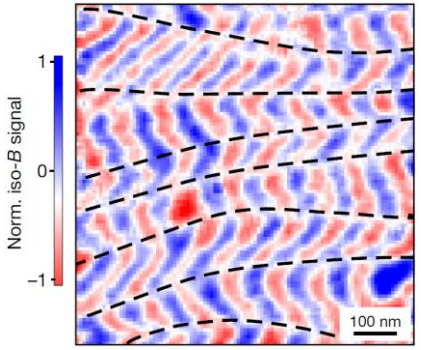

Rev. Sci. Instrum. **87**, 063703 (2016); Nature **549**, 252 (2017)

Outline

- **Basics of NV centers in diamond**
  - Structure
  - Optical & magnetic properties
- **Basics of magnetic resonance**
- **Quantum sensing**
  - AC magnetometry
  - Detection of proton spin ensemble
  - Detection and control of a single proton spin

Outline

- **Basics of NV centers in diamond**
  - Structure
  - Optical & magnetic properties
- **Basics of magnetic resonance**
- **Quantum sensing**
  - AC magnetometry
  - Detection of proton spin ensemble
  - Detection and control of a single proton spin

Crystal & energy level structures

- Negatively-charged (NV^-)
- 4 sp^3 orbitals, 6 e^- (5 from the defect, 1 captured)
- C_{3v} (symmetry axis = quantization axis)

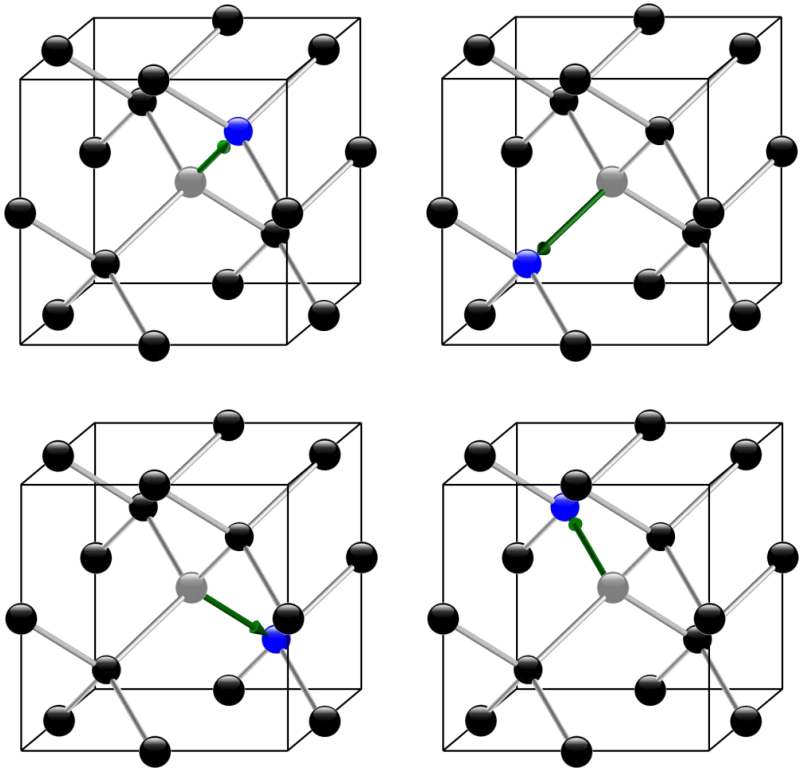

Effective spin-1 system
(e^2-hole spin-triplet)

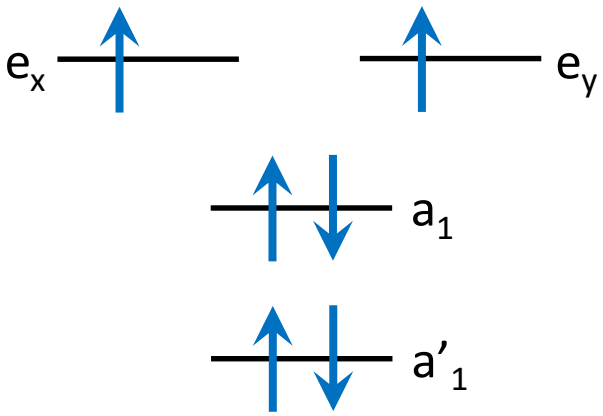

Energy levels

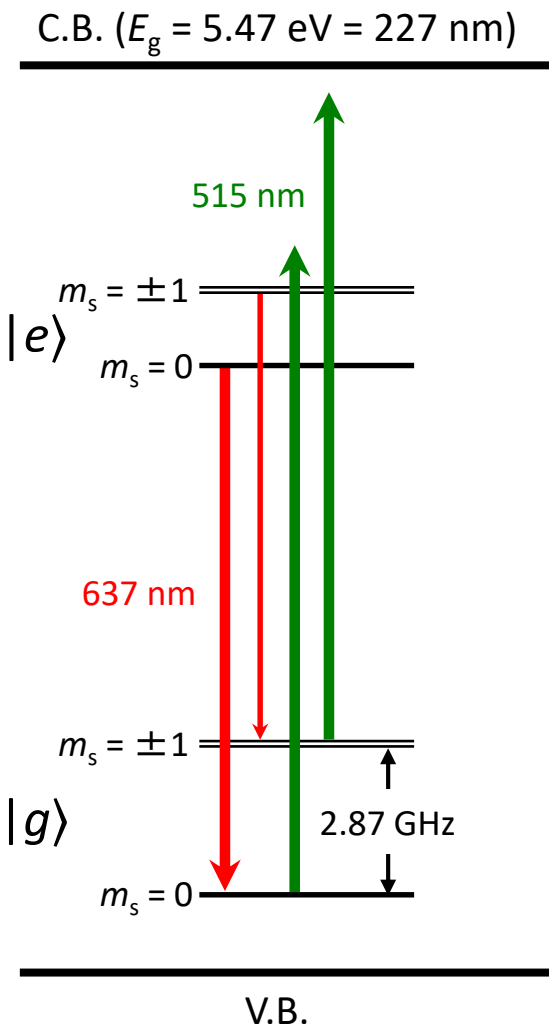

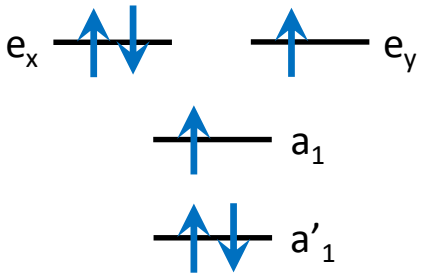

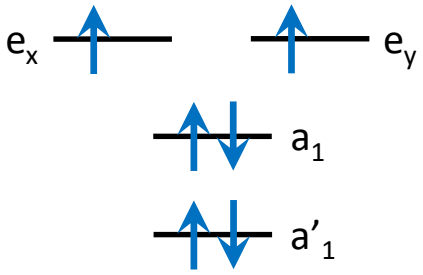

PL spectroscopy & imaging

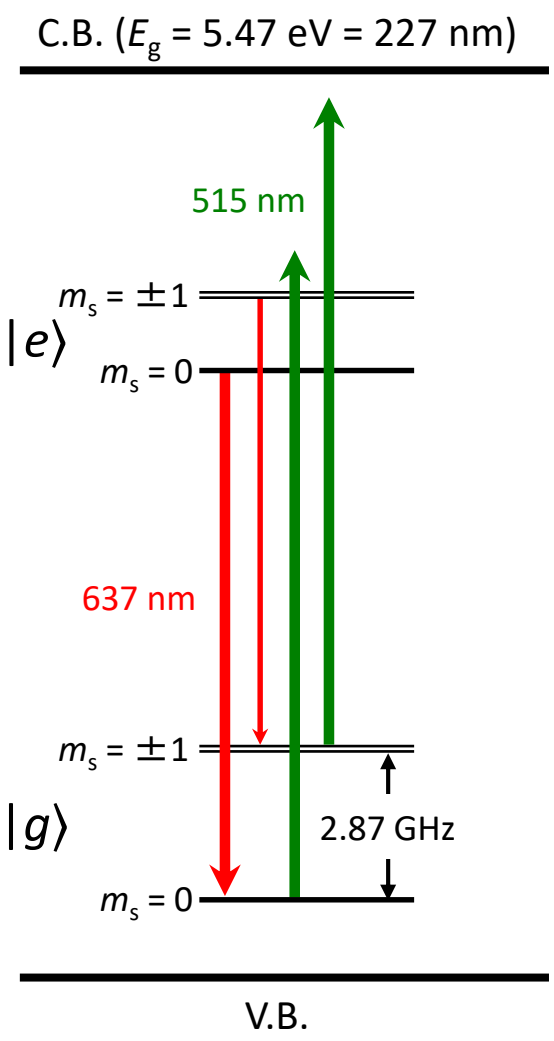

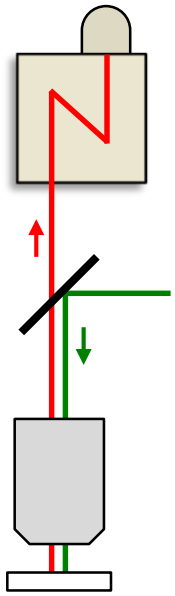

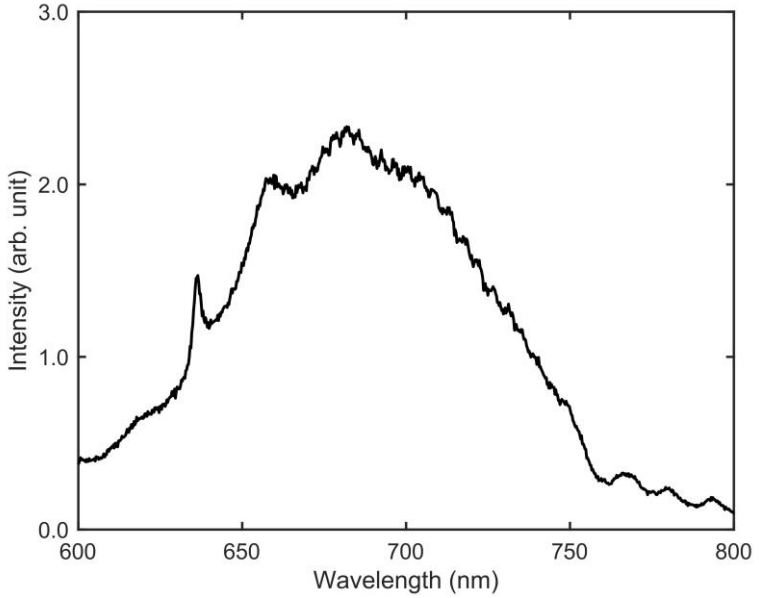

PL spectroscopy & imaging

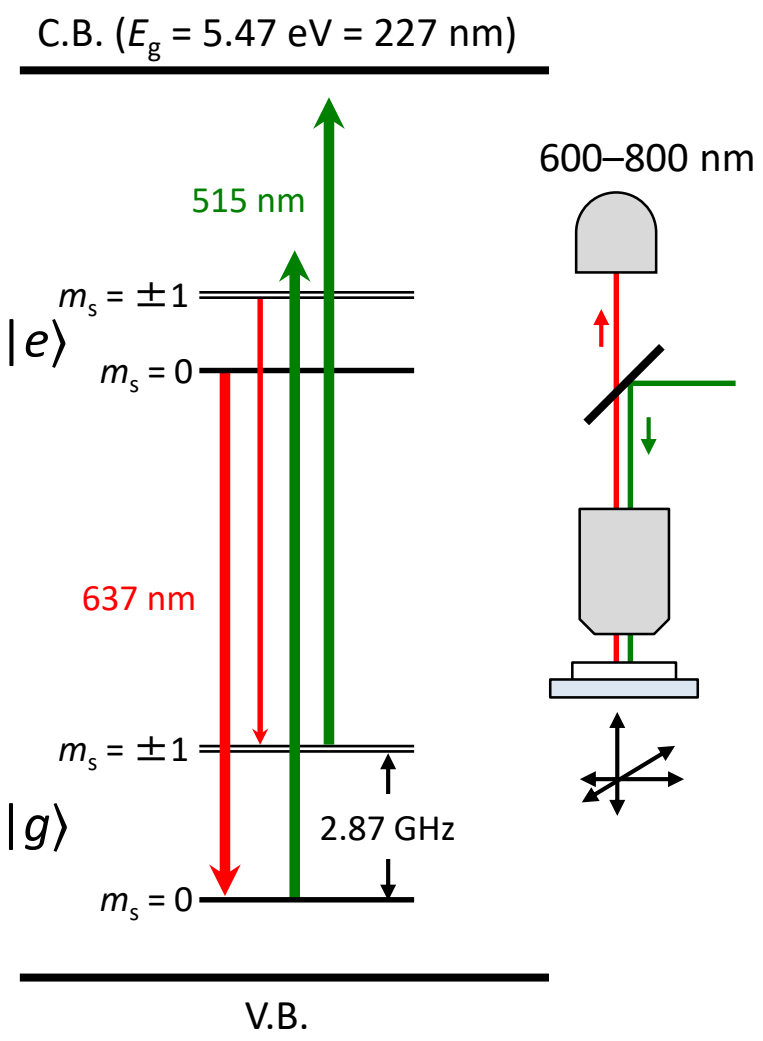

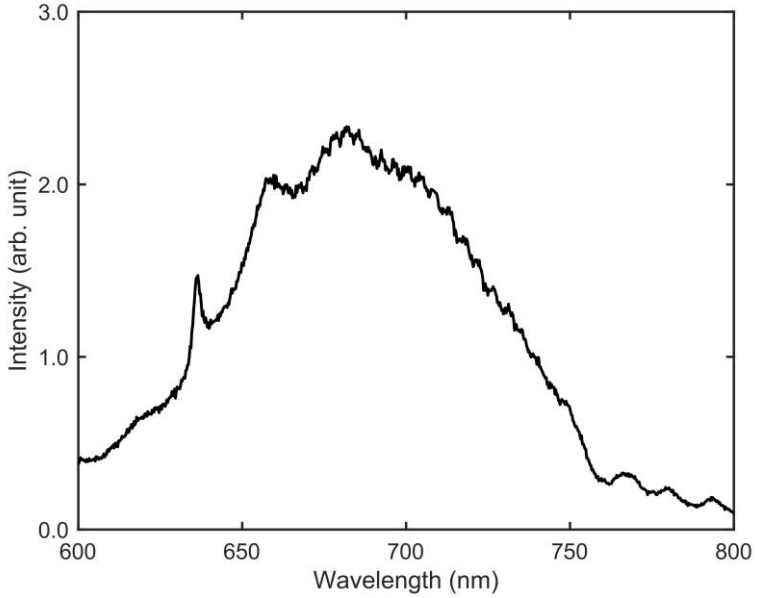

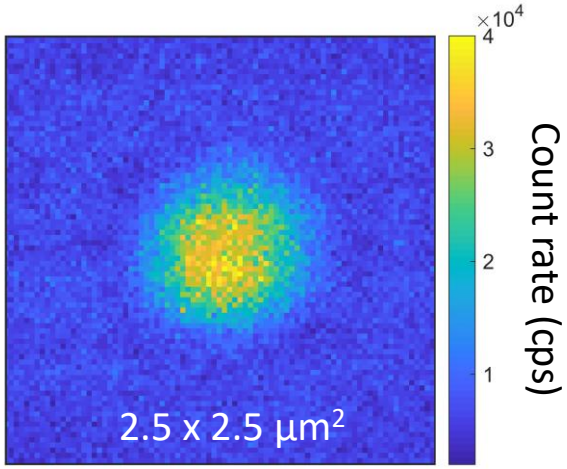

Photon statistics

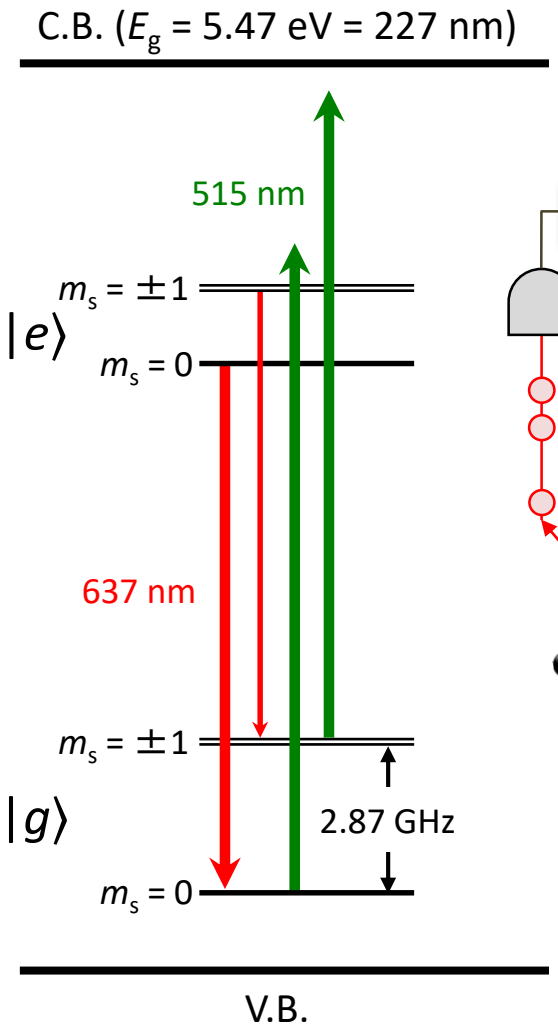

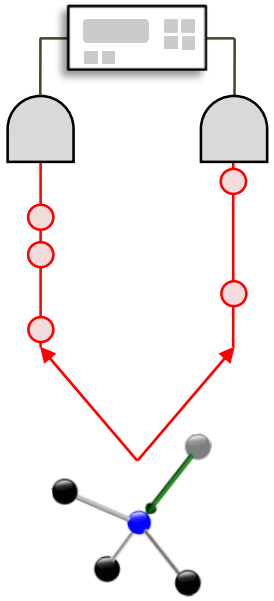

One photon at a time

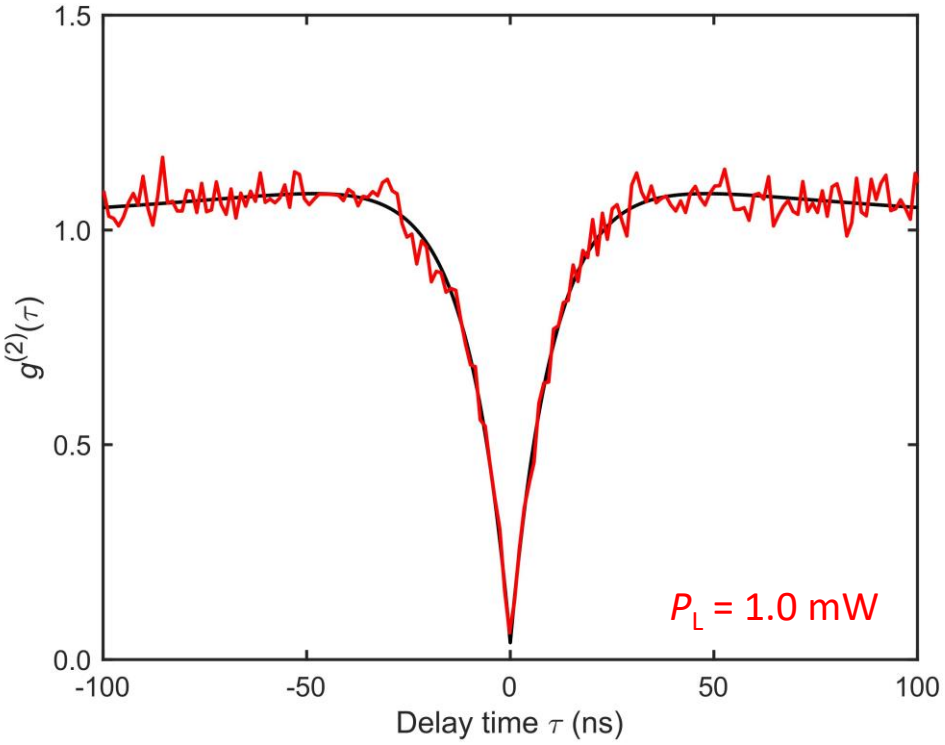

Time-resolved fluorescence

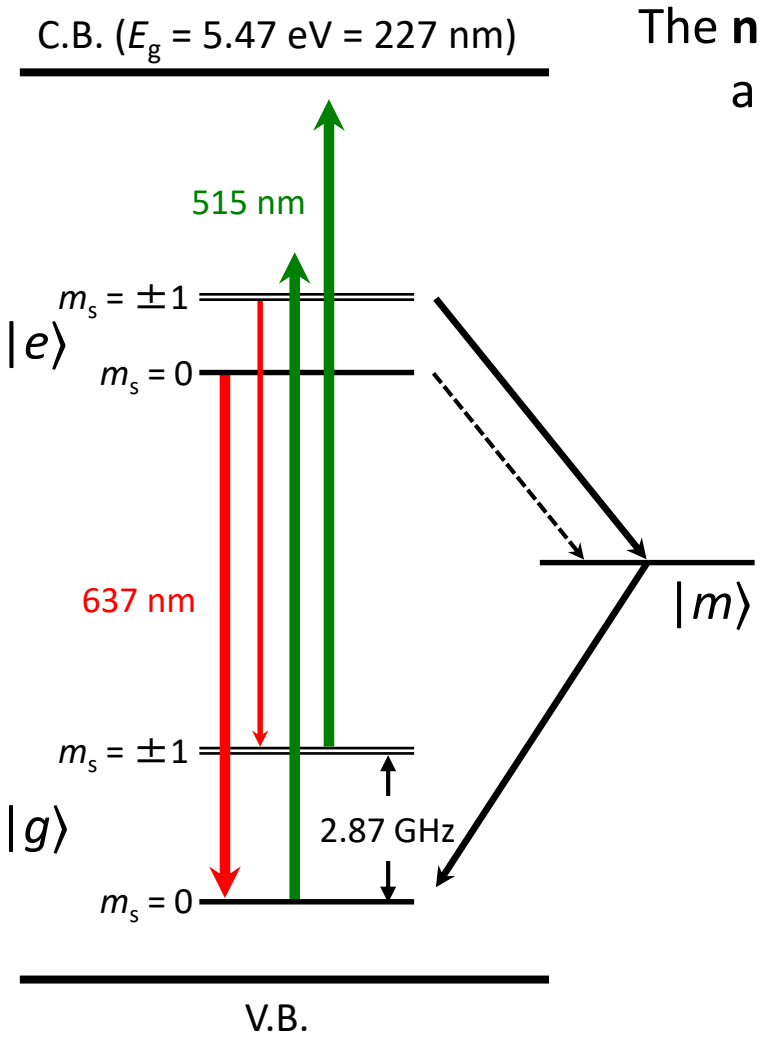

The **non-radiative** & **spin-selective** channel provides a means to **read out** & **initialize** the NV spin

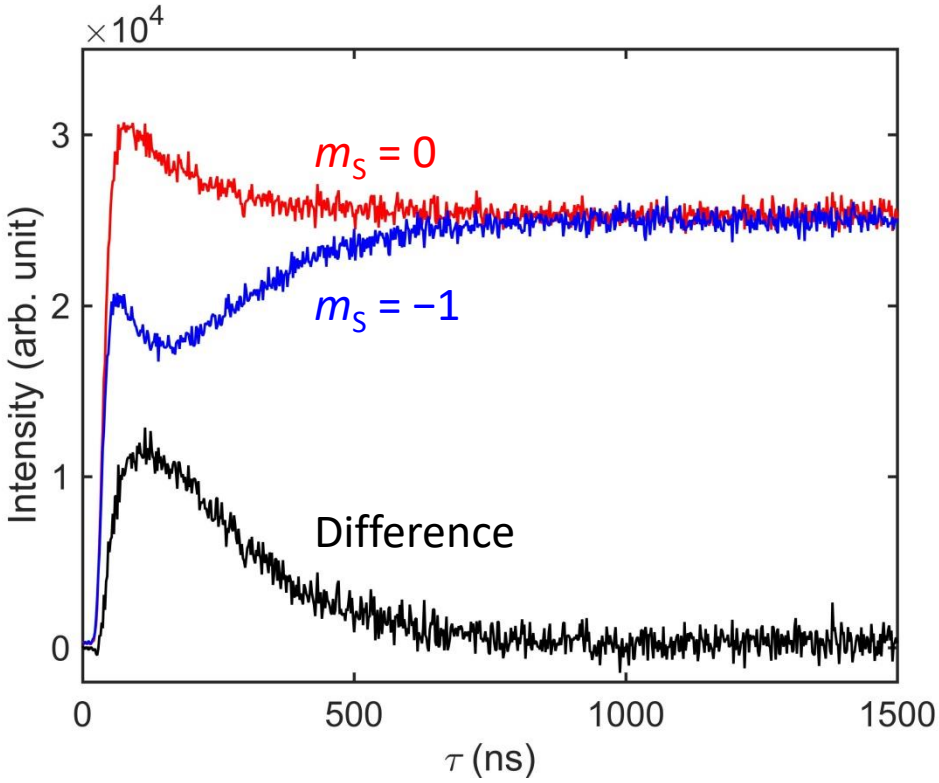

Optically detected magnetic resonance

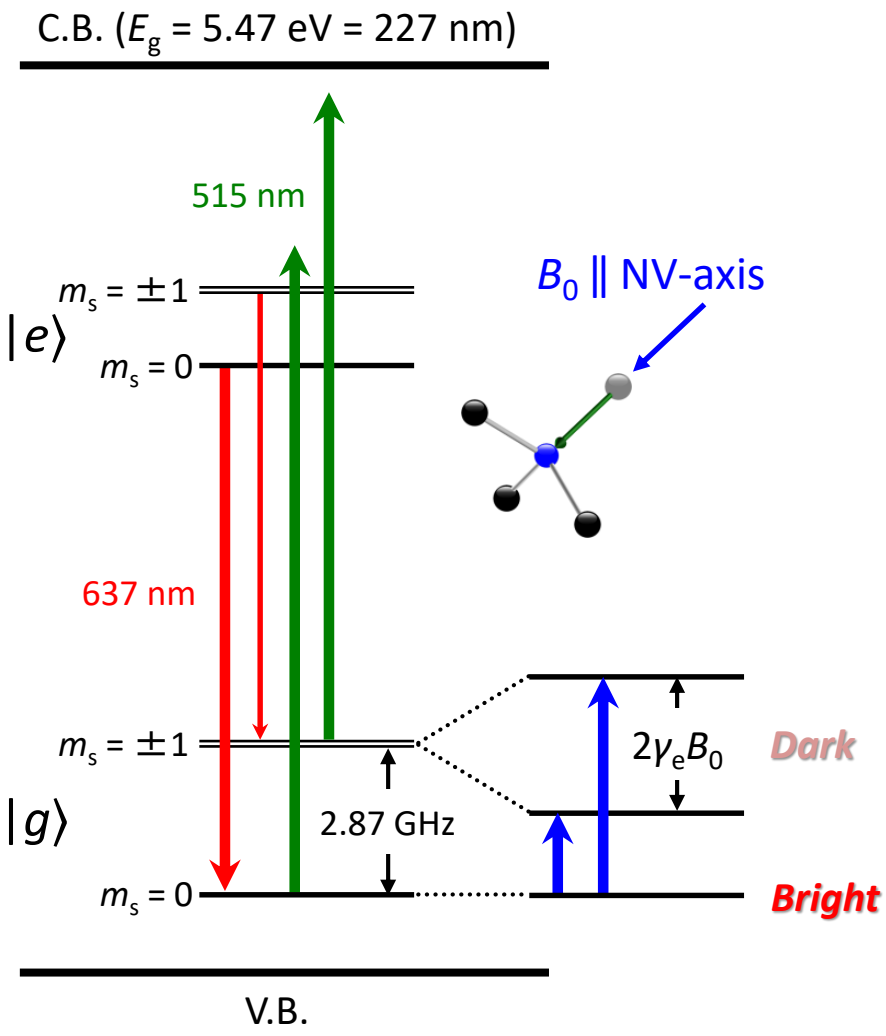

$$H = DS_z^2 + \gamma_e B_0 S_z$$

D = 2.87 GHz, γ_e = 28 MHz/mT

B_0 = 4.7 mT, $f_\pm$ = 2.87 ± 0.132 GHz

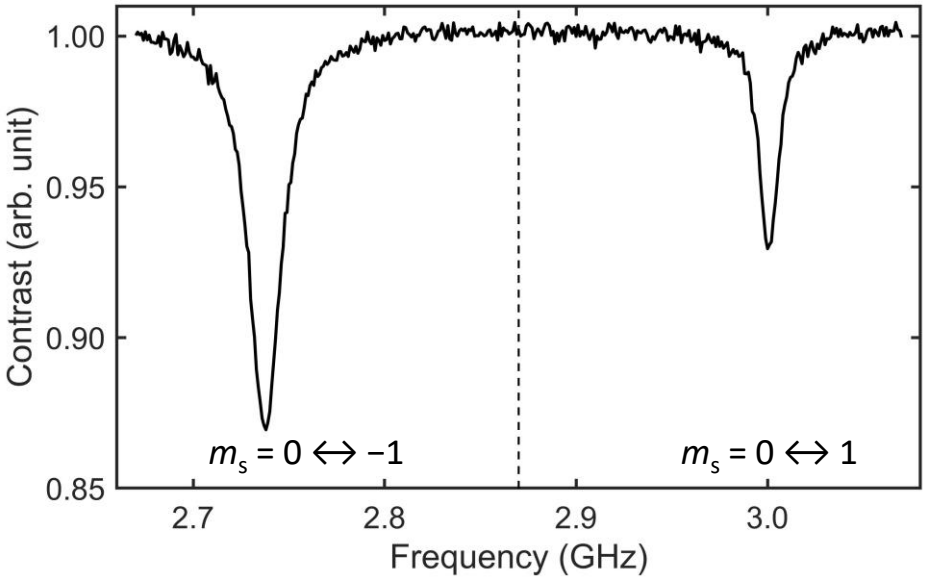

Experimental setup

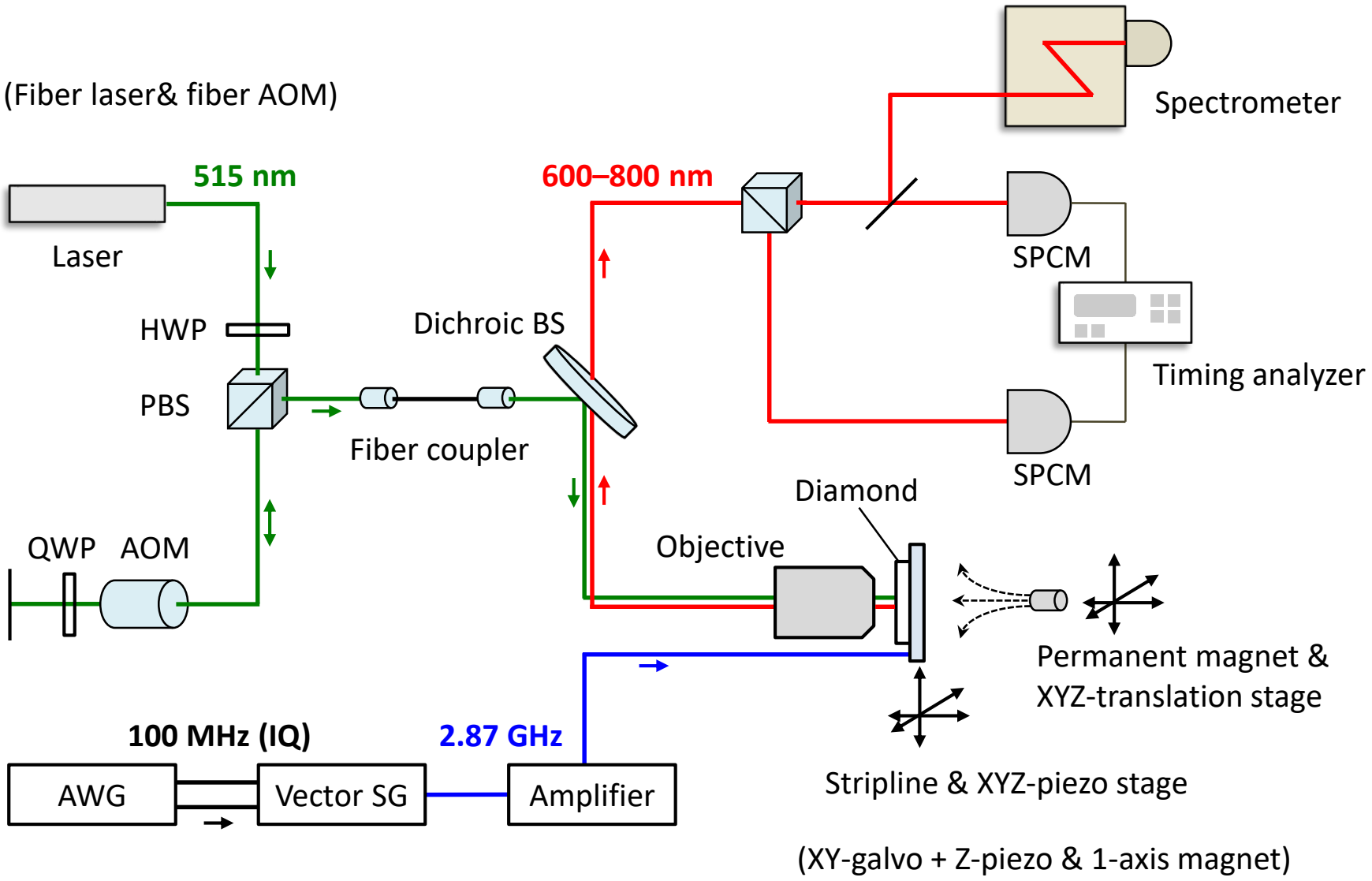

Experimental setup

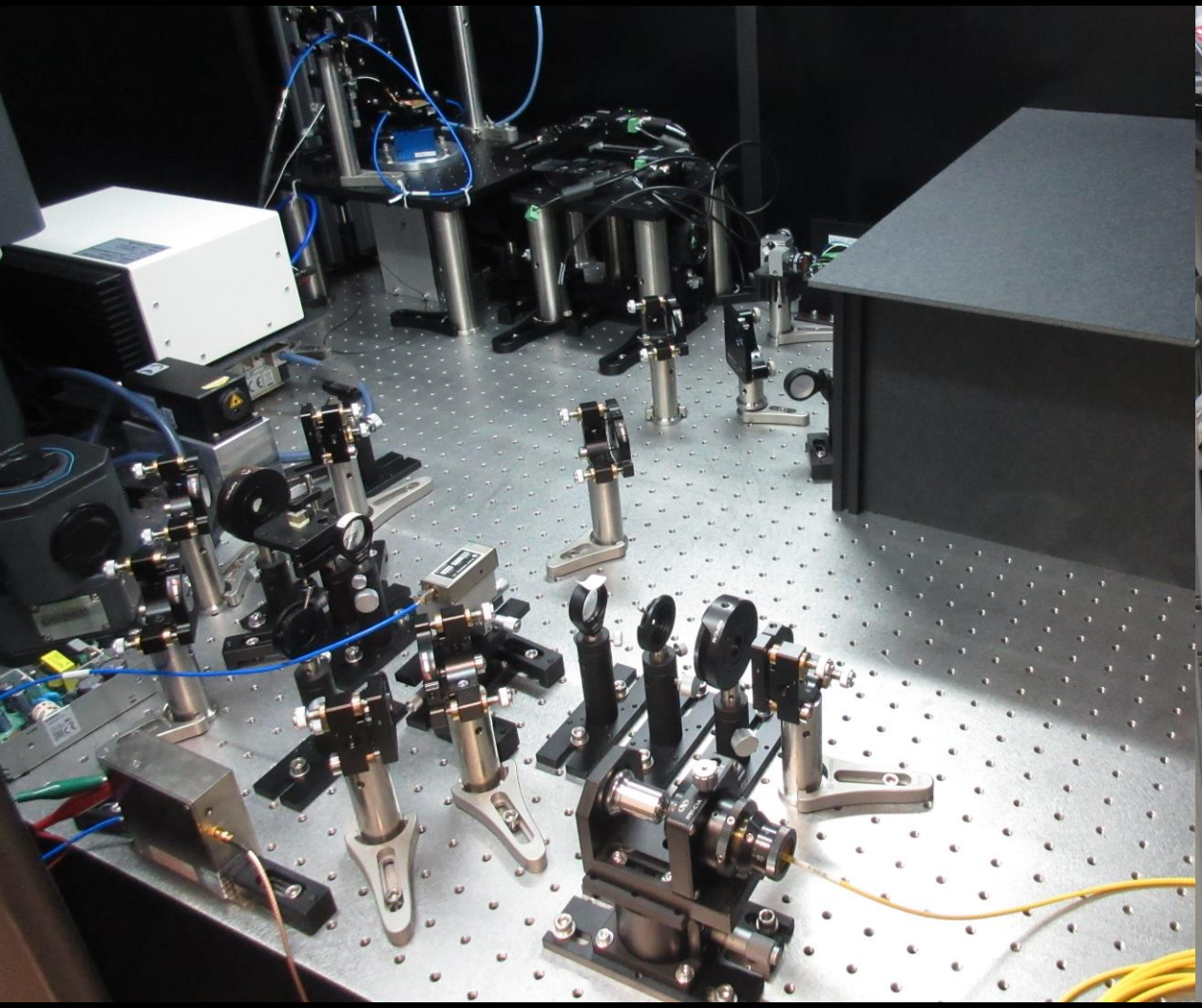

Experimental setup

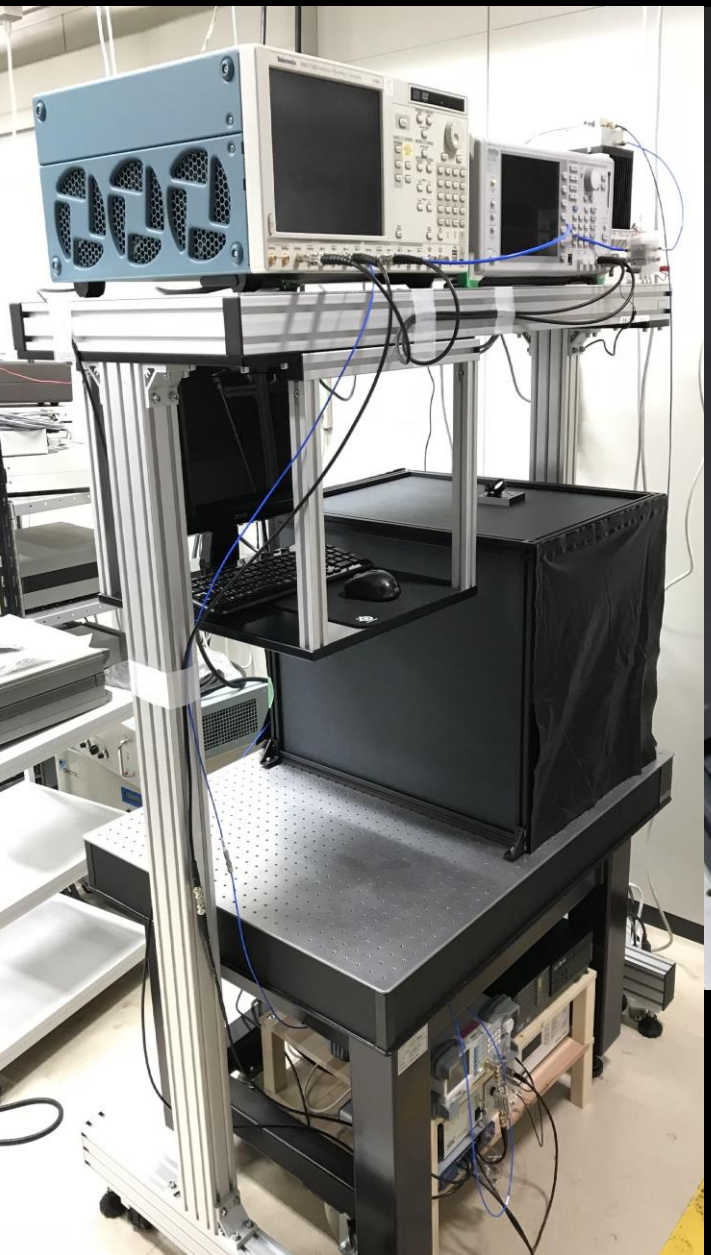

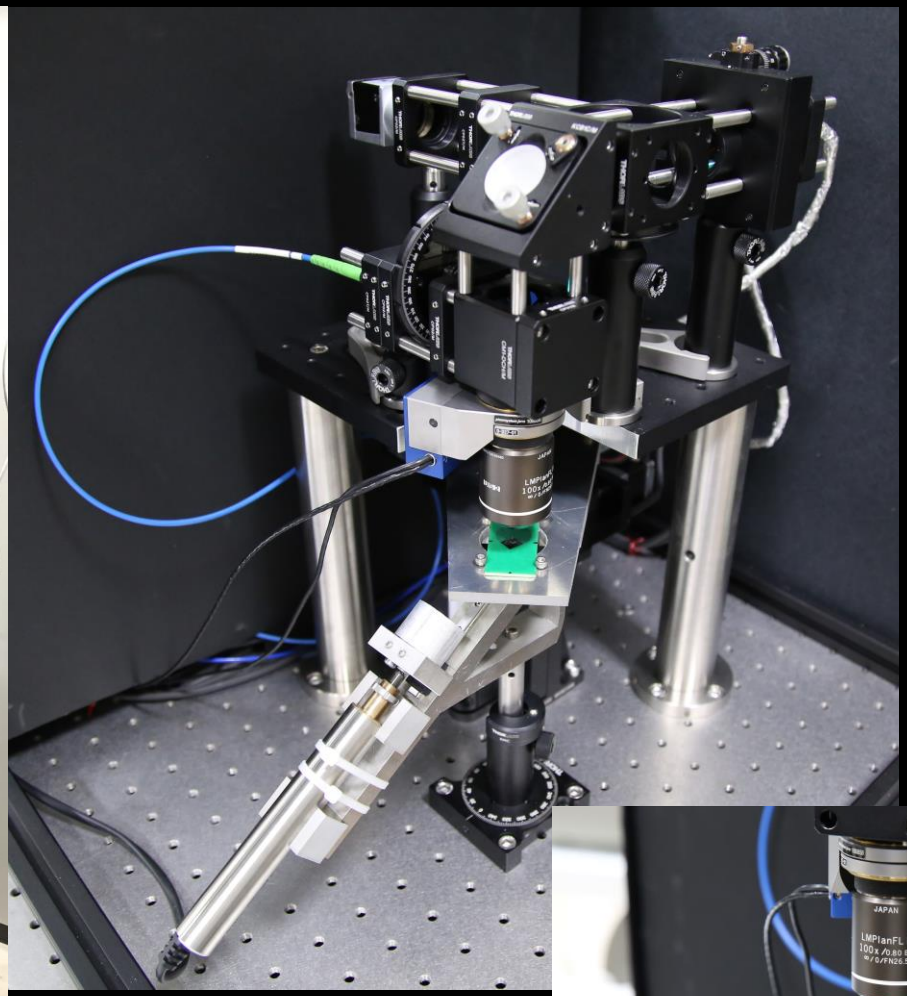

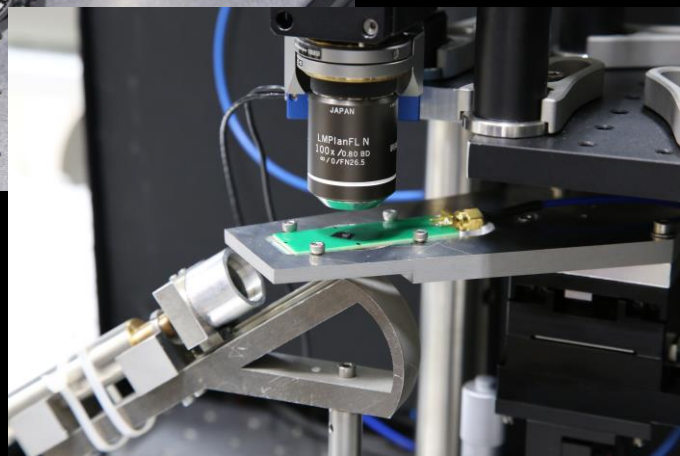

AIP Adv. **10**, 025206 (2020)
Misonou *et al.*

Outline

- **Basics of NV centers in diamond**
  - Structure
  - Optical & magnetic properties
- **Basics of magnetic resonance**
- **Quantum sensing**
  - AC magnetometry
  - Detection of proton spin ensemble
  - Detection and control of a single proton spin

Larmor precession

Torque equation

$$\frac{d\boldsymbol{\mu}}{dt} = \boldsymbol{\mu} \times \gamma \boldsymbol{B}_0$$

Gyromagnetic ratio ($g\mu_B$)

Magnetic moment: $\boldsymbol{\mu} = \gamma \boldsymbol{J}$

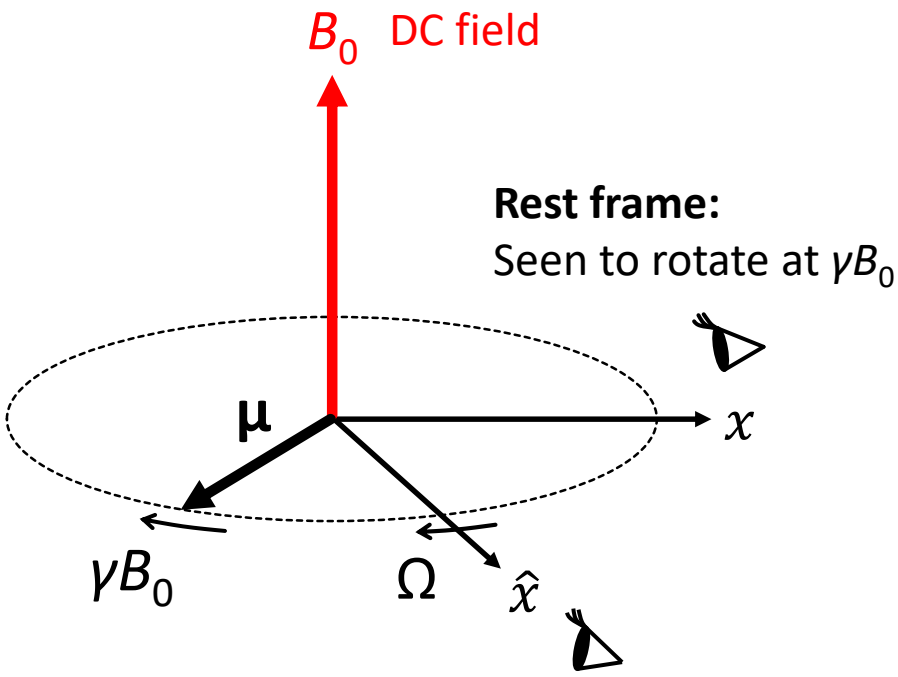

Frame rotating at angular velocity Ω:
Rotate slower…why?

Larmor precession

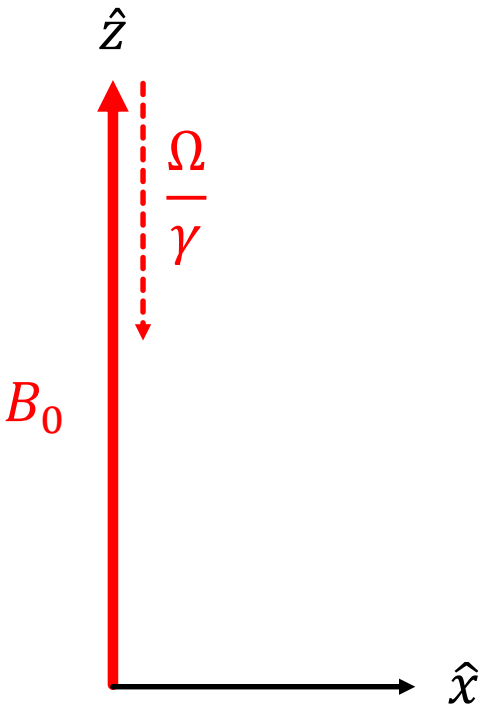

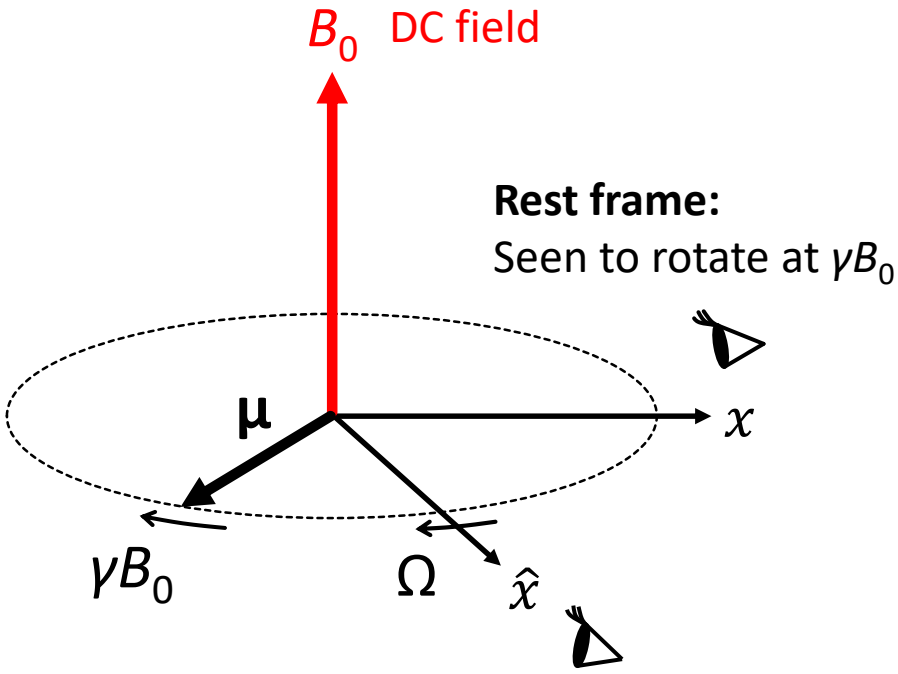

Frame rotating at angular velocity Ω:
Rotate slower…why?

DC field along the *z* direction becomes weaker

Magnetic resonance

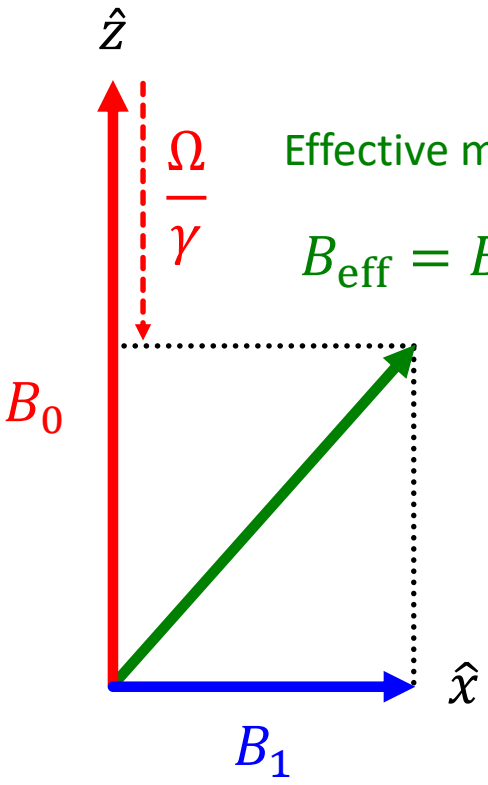

Effective magnetic field

$$B_{\text{eff}} = B_1\hat{x} + \left(B_0 - \frac{\Omega}{\gamma}\right)\hat{z}$$

AC field rotating in the *xy* plane at Ω

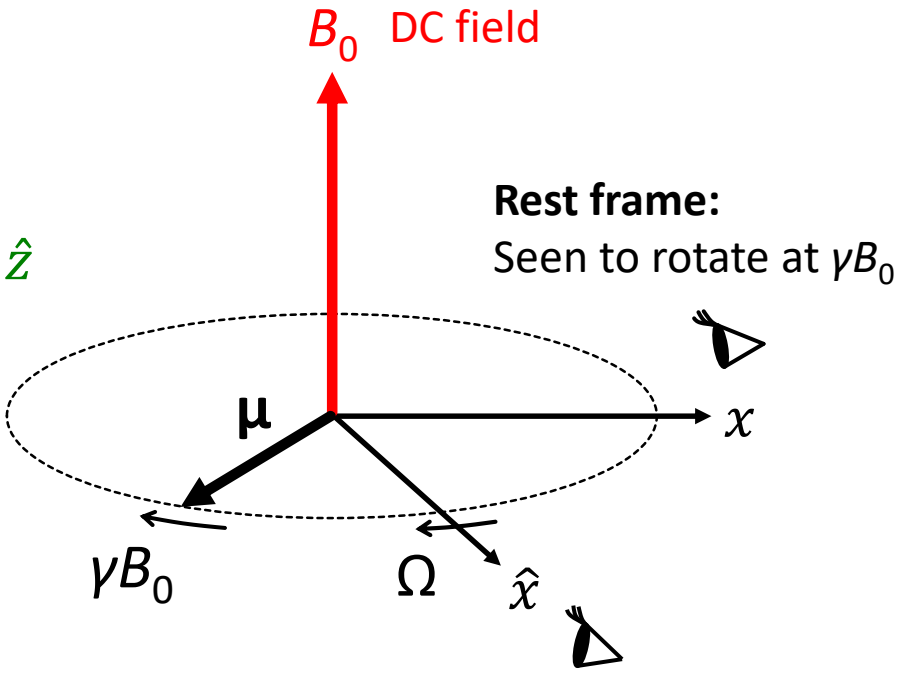

Frame rotating at angular velocity Ω:
Rotate slower…why?

DC field along the *z* direction becomes weaker

Magnetic resonance

Frame rotating at Ω = γB_0

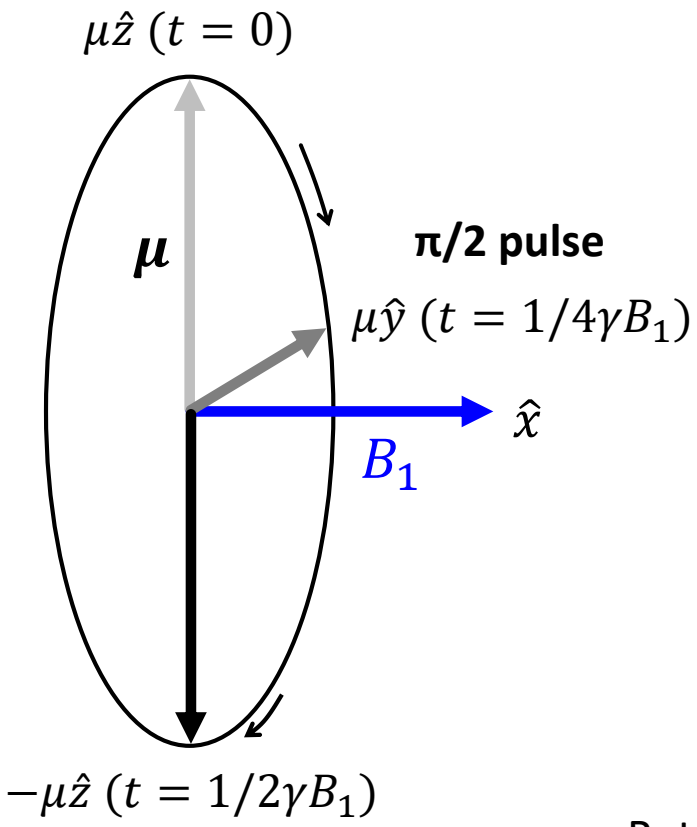

Rest (non-resonant) frame

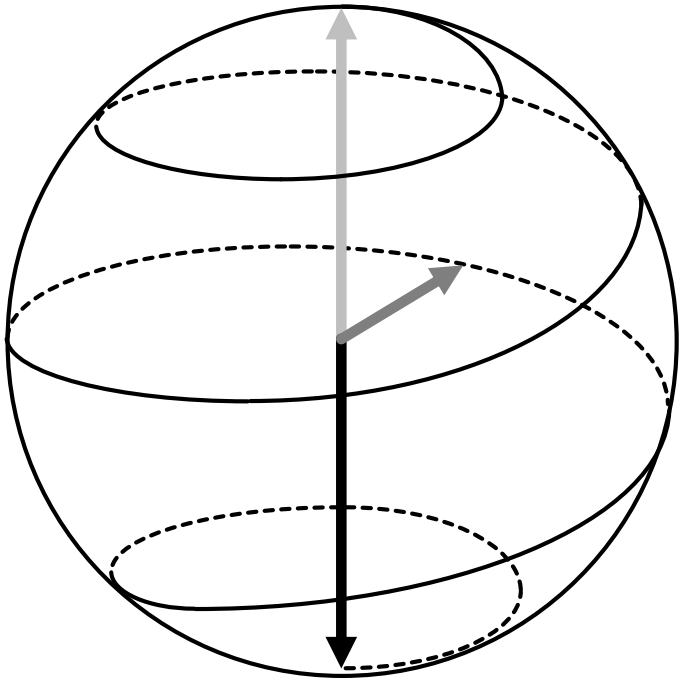

- Rotations about the $\pm\hat{x}, \pm\hat{y}$ axes are realized by adjusting the microwave phases
- Rotation about the $\hat{z}$ axis is superposed when observed from the rest (non-resonant) frame

Qubit & Bloch sphere

Qubit, spin-½ (NV is spin-1!)

$$\begin{cases} |"0"\rangle \equiv |m_s = 0\rangle \\ |"1"\rangle \equiv |m_s = -1\rangle \end{cases}$$

$$|\psi\rangle = \cos\frac{\theta}{2}|0\rangle + e^{i\phi}\sin\frac{\theta}{2}|1\rangle$$

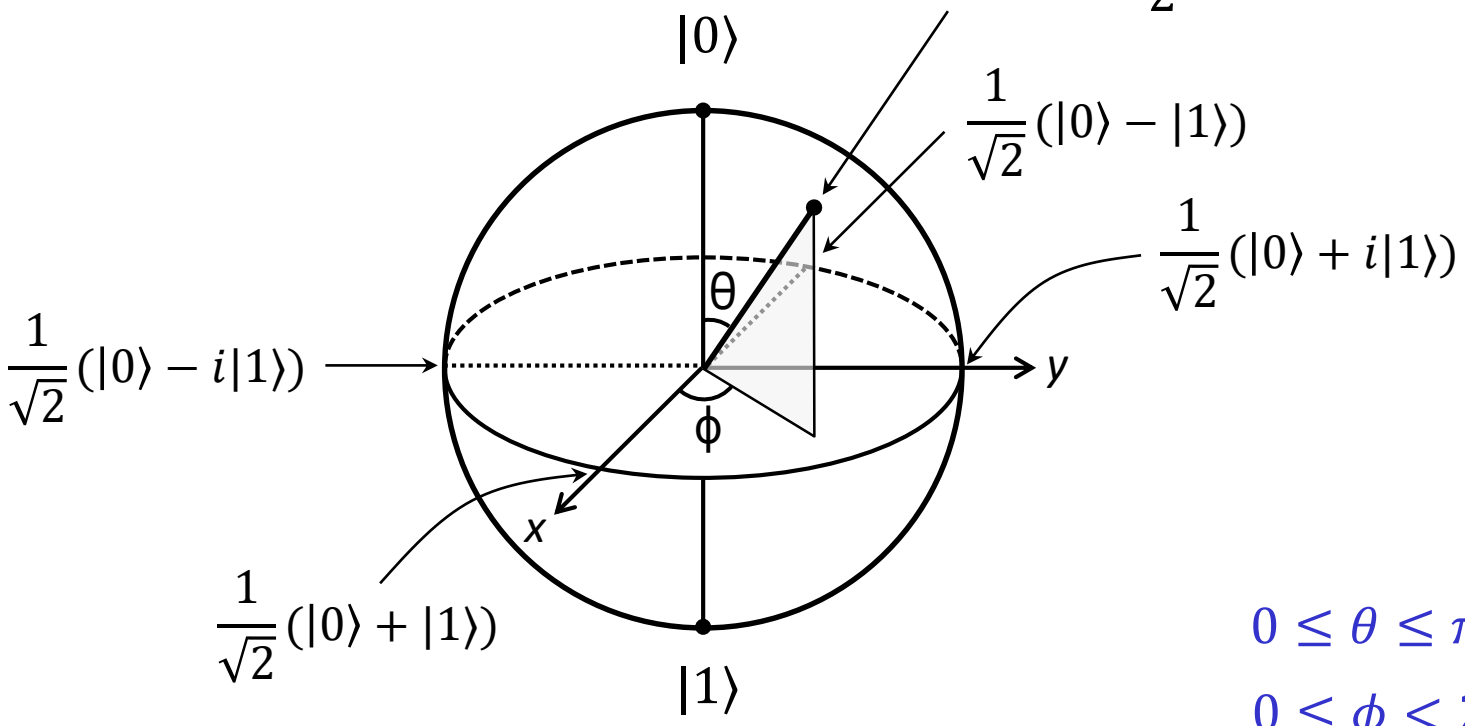

$$0 \le \theta \le \pi$$

$$0 \le \phi < 2\pi$$

Rabi oscillation

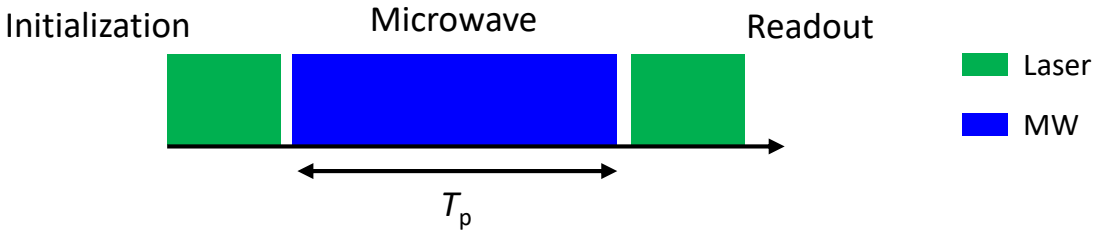

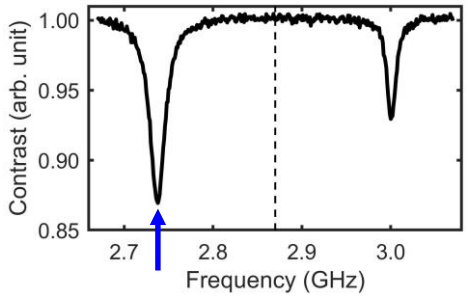

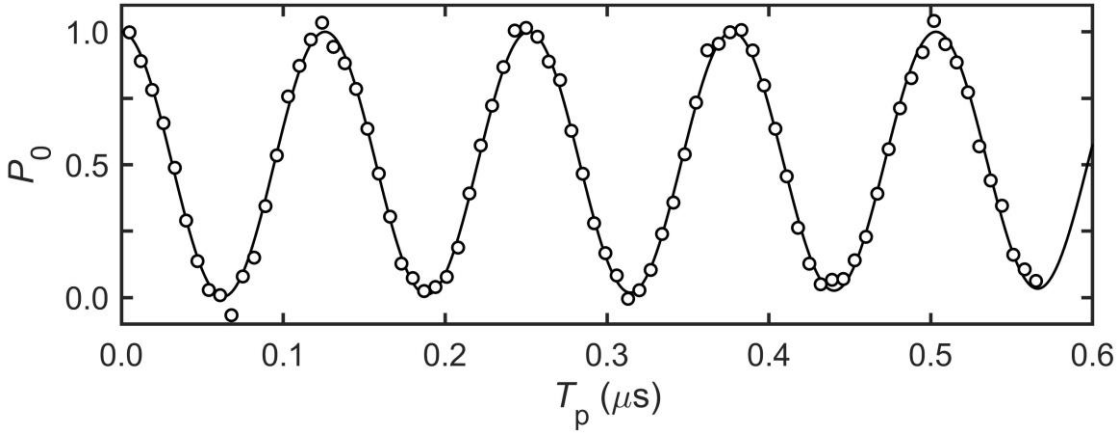

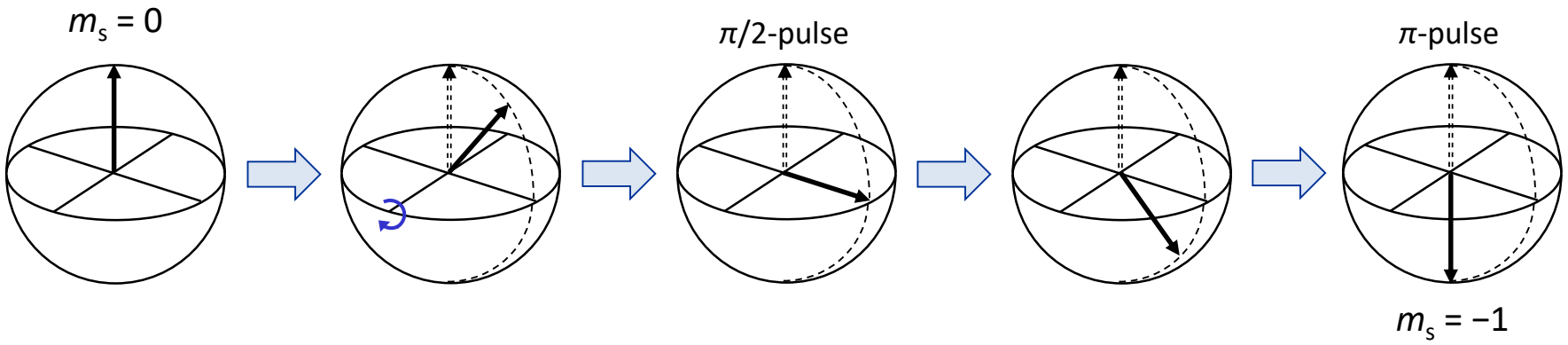

Quantum coherence

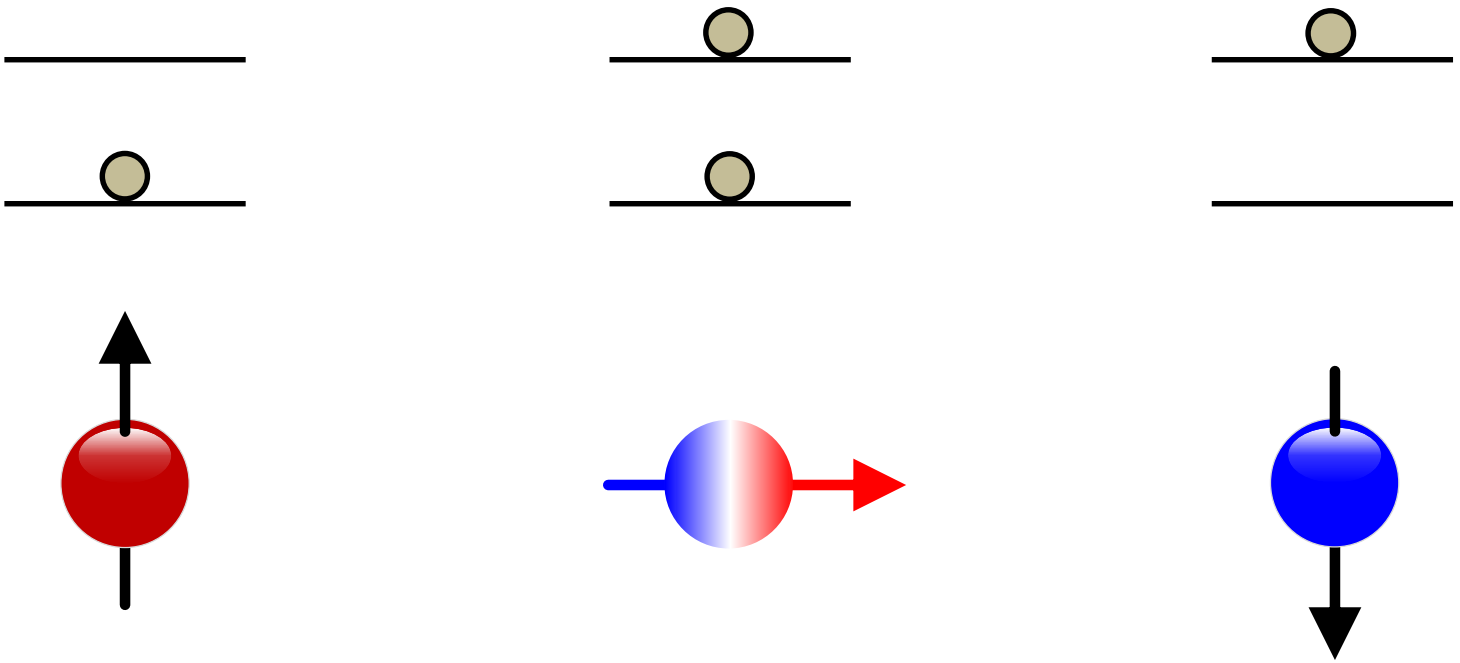

$|0\rangle \equiv |m_s = 0\rangle$ $|\Psi\rangle = \alpha|0\rangle + \beta|1\rangle$ $|1\rangle \equiv |m_s = -1\rangle$

T_2: measure of how long a superposition state is preserved

Relaxation: T_1 & T_2

Bloch equation

$$\frac{d\boldsymbol{\mu}}{dt} = \boldsymbol{\mu} \times \gamma \boldsymbol{B}_0 - \frac{\boldsymbol{\mu}_{\parallel} - \boldsymbol{\mu}_0}{T_1} - \frac{\boldsymbol{\mu}_{\perp}}{T_2}$$

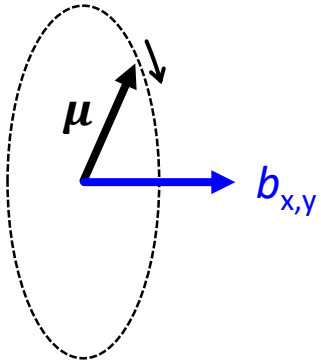

Energy relaxation (Change the direction of a spin)

$$\frac{1}{T_1} = \frac{\gamma^2}{2} \int_{-\infty}^{\infty} \left[\langle b_x(\tau) b_x(0) \rangle + \langle b_y(\tau) b_y(0) \rangle \right] \cos(\omega_0 \tau)\, d\tau$$

Phase relaxation (Change the precession frequency)

$$\frac{1}{T_2} = \frac{1}{2T_1} + \frac{\gamma^2}{2} \int_{-\infty}^{\infty} \langle b_z(\tau) b_z(0) \rangle d\tau$$

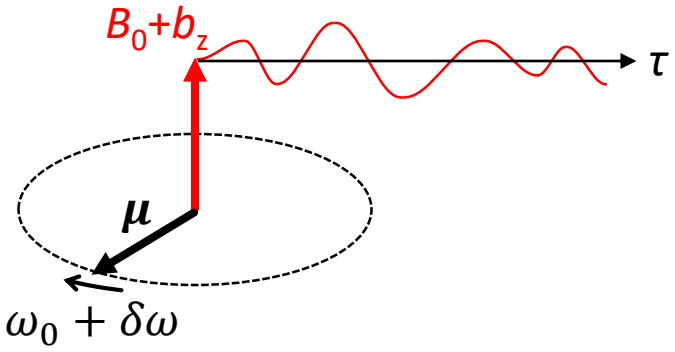

→ Incoherent process

Relaxation: T_1 & T_2

Bloch equation

$$\frac{d\boldsymbol{\mu}}{dt} = \boldsymbol{\mu} \times \gamma \boldsymbol{B}_0 - \frac{\boldsymbol{\mu}_{\parallel} - \boldsymbol{\mu}_0}{T_1} - \frac{\boldsymbol{\mu}_{\perp}}{T_2}$$

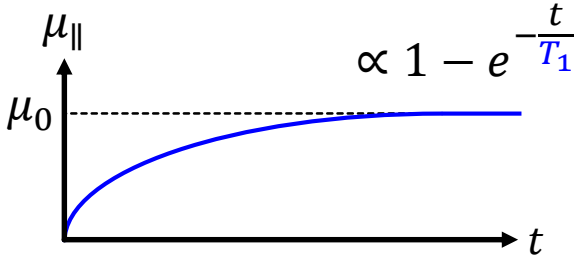

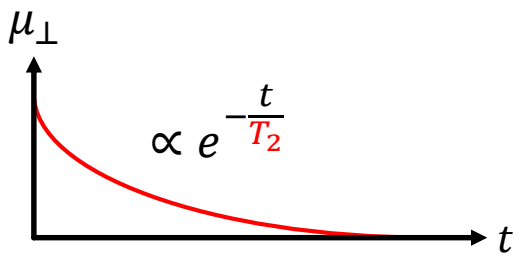

In typical spin systems, T_2 is much shorter than T_1

Measurement of T_2

Time domain → Decay time constant T_2

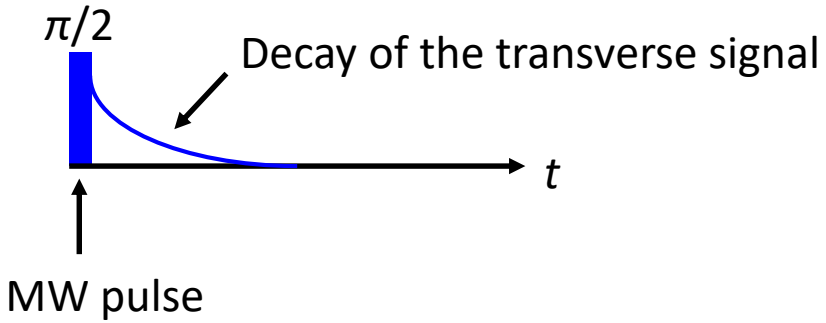

Frequency domain → Lorentz width

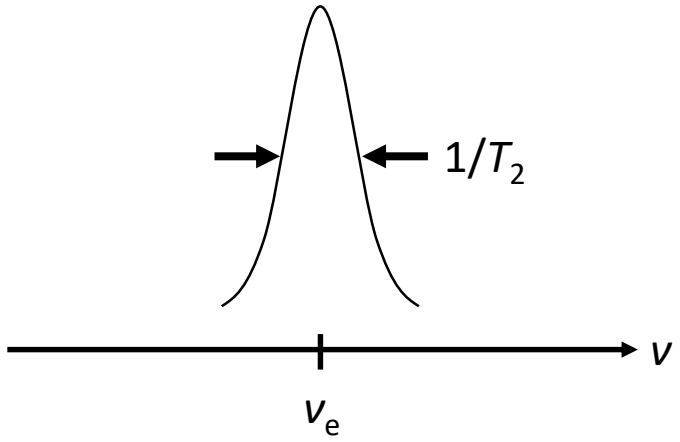

Measurement of T_2

Time domain → Decay time constant T_2

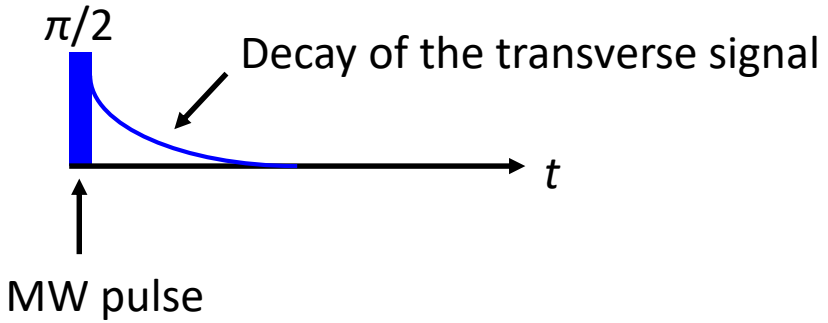

Frequency domain → Lorentz width

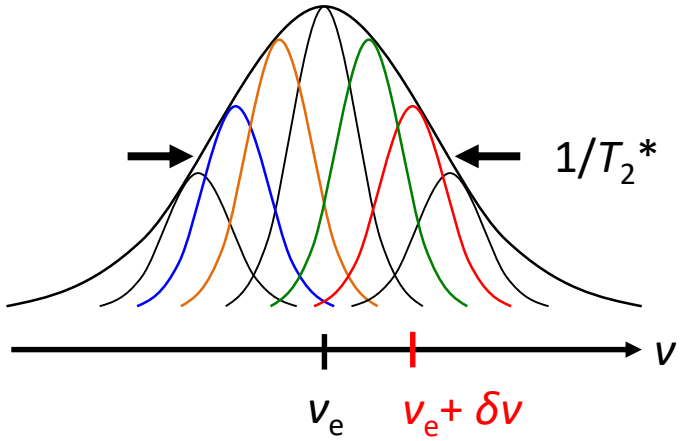

Inhomogeneous line broadening

Seen to precess at $\delta\nu$ in the frame rotating at ν_e

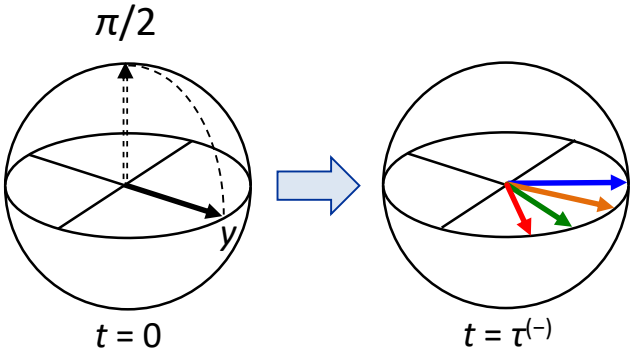

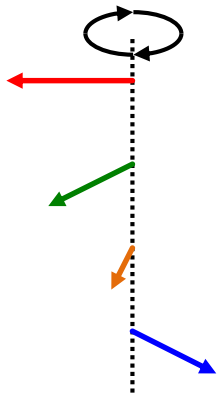

Spin echo

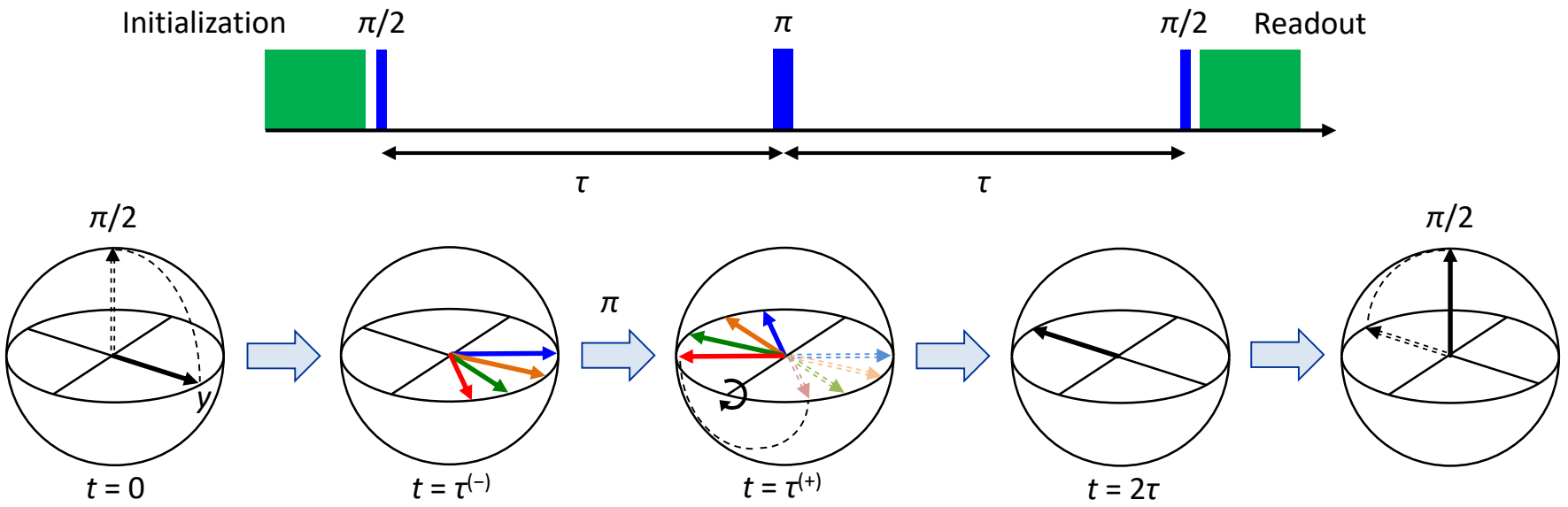

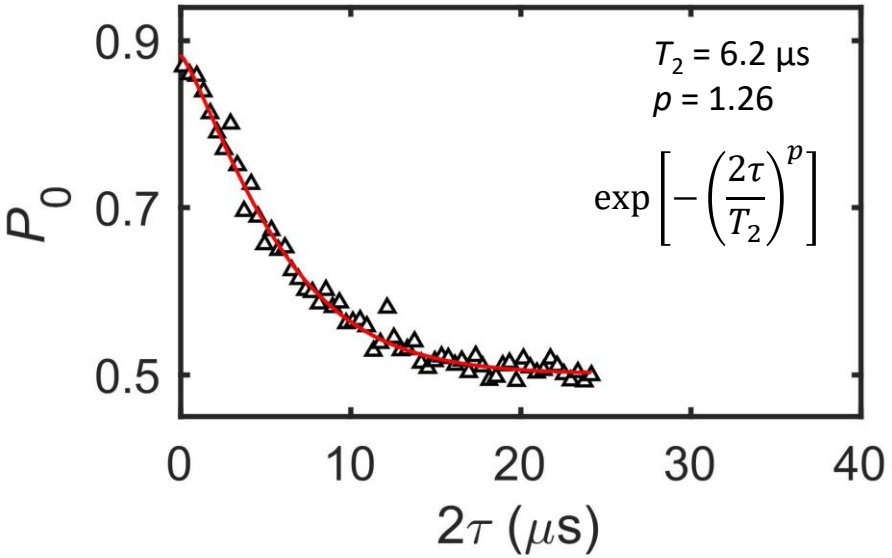

Static DC shifts cancelled (refocusing)

Near-surface NV center

- N^+ implantation into ^{12}C (I = 0) layer
- d_{NV} = 6.26 nm
- B_0 = 23.5 mT

AIP Adv. **10**, 025206 (2020) Misonou *et al.*

Outline

- **Basics of NV centers in diamond**
  - Structure
  - Optical & magnetic properties
- **Basics of magnetic resonance**
- **Quantum sensing**
  - AC magnetometry
  - Detection of proton spin ensemble
  - Detection and control of a single proton spin

Quantum sensing of nuclear spins

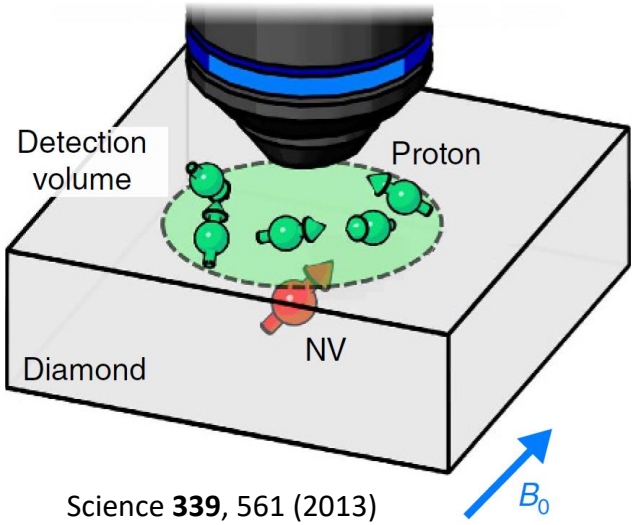

Science **339**, 561 (2013)

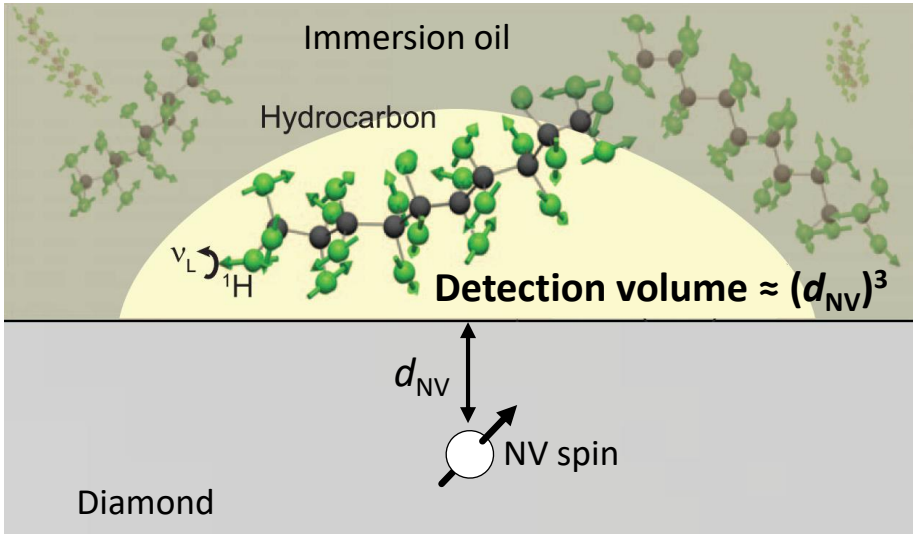

Nature Commun. **6**, 8527 (2015)

Nuclear spins **precess** at f_{ac} = a few kHz–MHz under B_0

⇨ **Weak AC magnetic field** on the NV spin

⇨ Detect using **quantum coherence** of the NV spin

AC magnetometry

$N = 4$

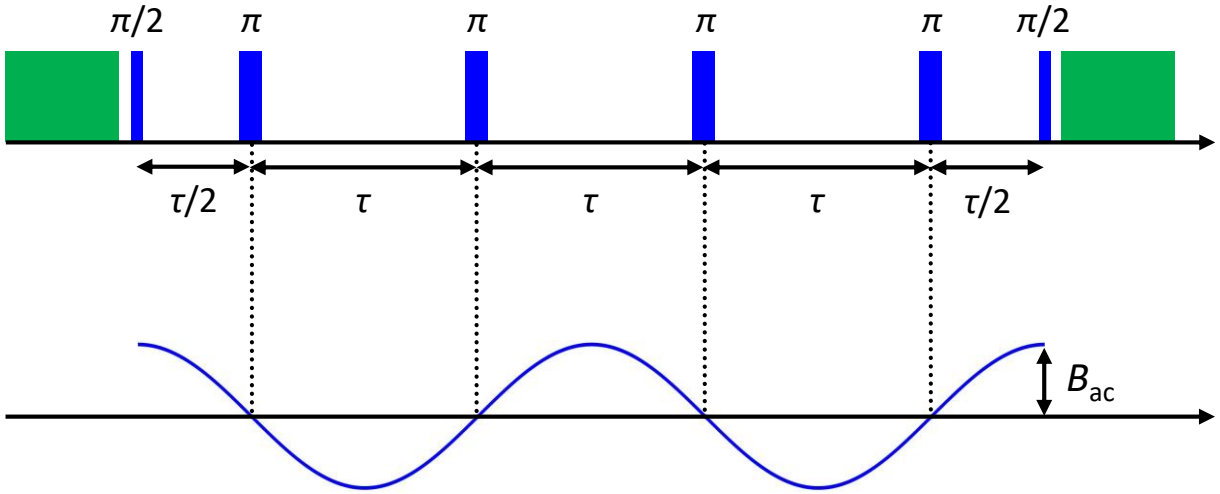

AC field
($f_{ac} = 1/2\tau$)

Sensor phase buildup (deviation from *y* axis): *loss of coherence*

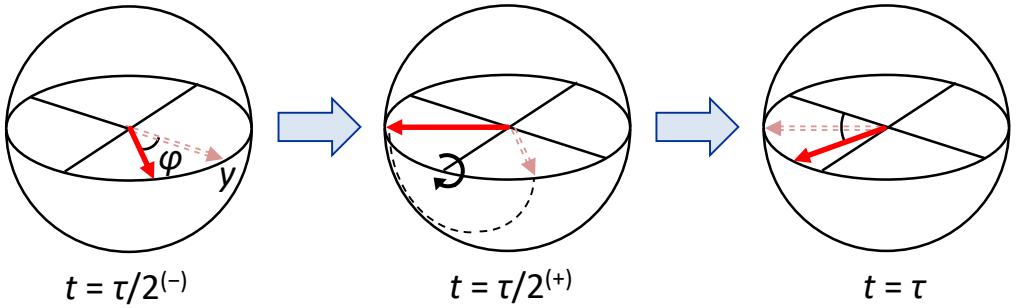

$\varphi(\tau) = 2\varphi(\tau/2)$

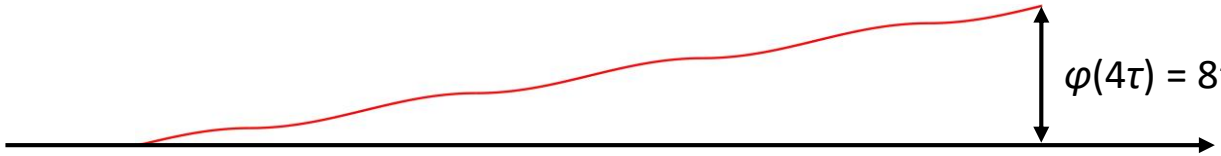

AC magnetometry

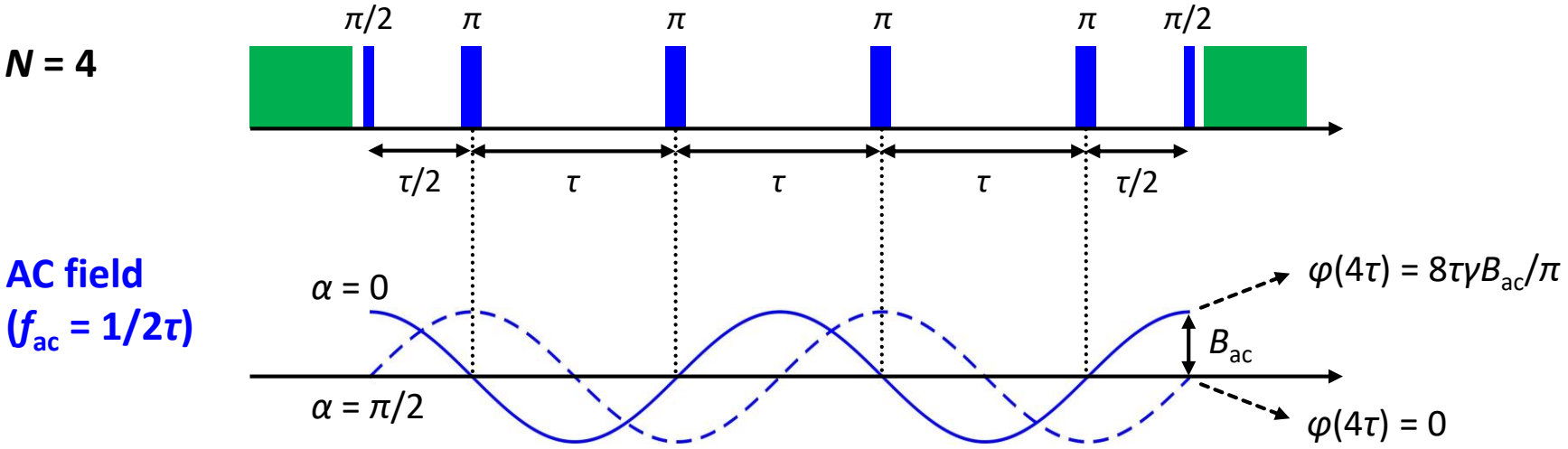

Sensor phase buildup (deviation from *y* axis): *the initial phase α matters*

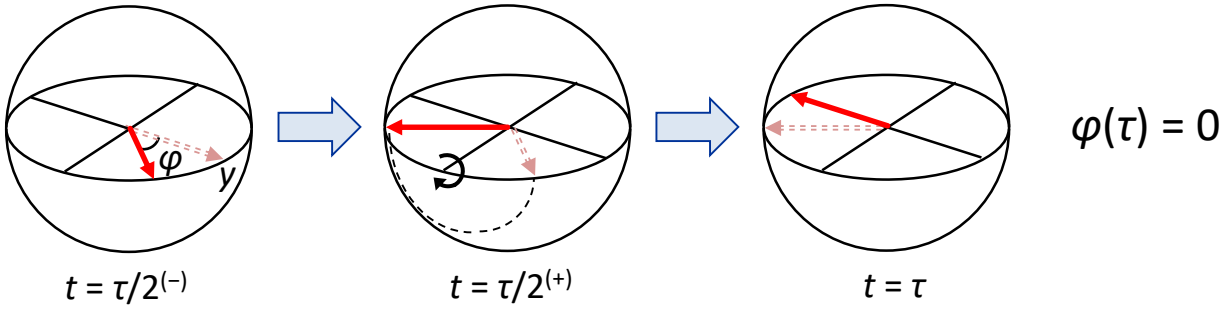

- $\varphi \propto \cos\alpha$
- Usually, we average over **random *α***

Sensing of ensemble *n*-spins

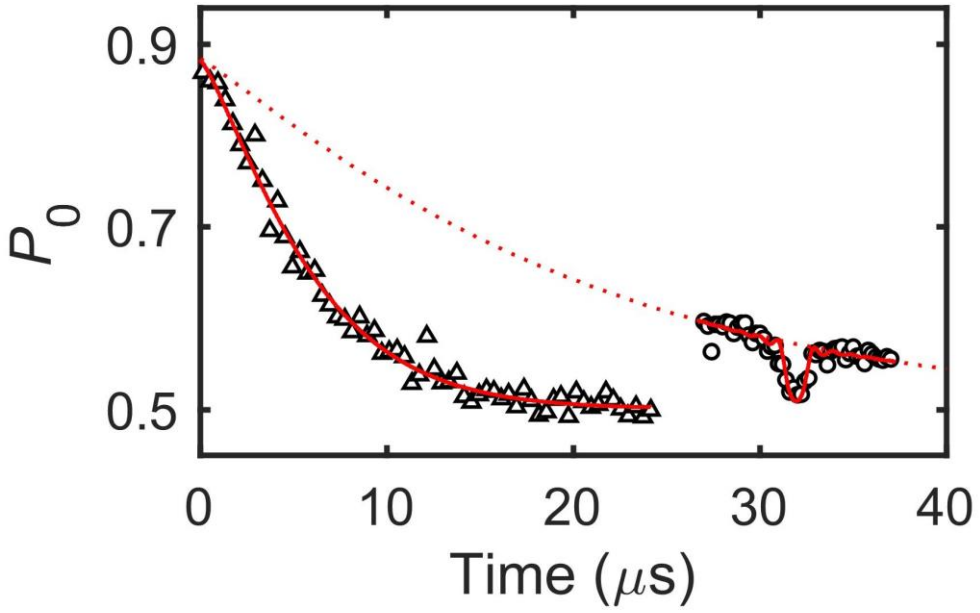

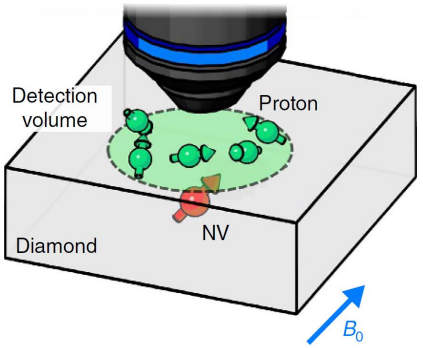

- T_2 = 6.2 µs @B_0 = 23.5 mT
- N = 64
- 2τ = 2 x 32 µs/64 = 1 µs
  → $\gamma_H B_0$ = (42.577 kHz/mT) x B_0 = 1.00 MHz

AIP Adv. **10**, 025206 (2020) Misonou *et al.*

Sensing of ensemble *n*-spins

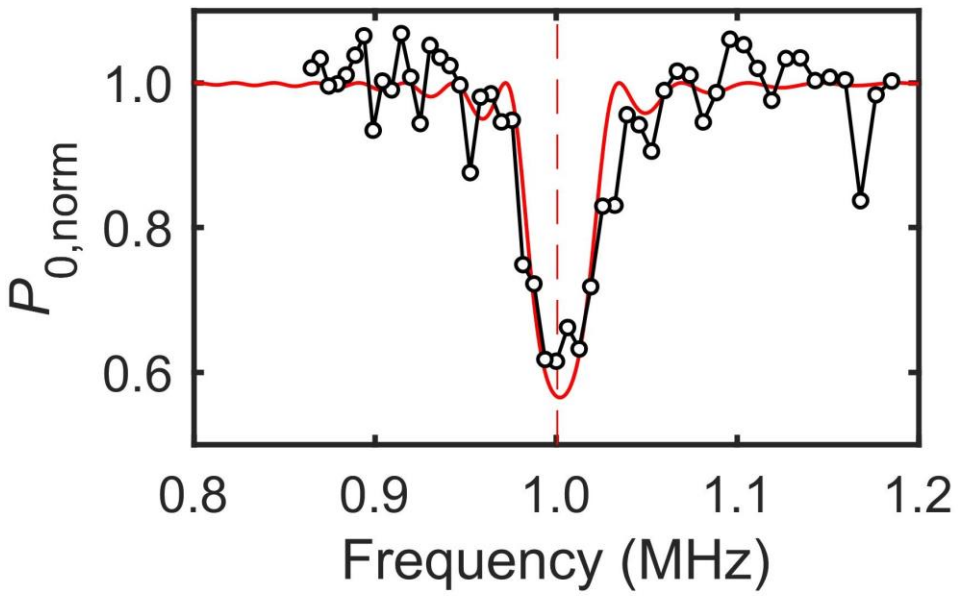

$$C(\tau) = f(B_{\mathrm{rms}})$$

$$B_{\mathrm{rms}} = \frac{\mu_0}{4\pi} h\gamma_{\mathrm{H}} \sqrt{\frac{5\pi\rho}{96 d_{\mathrm{NV}}^3}}$$

Phys. Rev. B **93**, 045425 (2016)

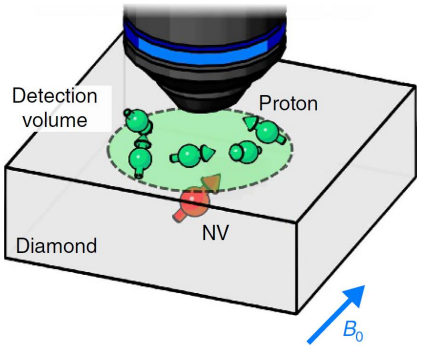

- Proton density ρ = 6 x 10^{28} m^{-3} (known)
- d_{NV} = 6.26 nm
- B_{rms} ≈ 560 nT
- Detection volume $(d_{NV})^3$ ≈ **0.25 zL** (zepto = 10^{-21})
- # of protons $\rho(d_{NV})^3$ ≈ 1500
- Thermal polarization (10^{-7}) vs. statistical fluctuation $(1500)^{0.5}$ ≈ **39**

AIP Adv. **10**, 025206 (2020) Misonou *et al.*

Toward single-molecular imaging

- **High spatial resolution**
  - → Special about *single-nuclear-spin-level* NMR
  - → Measure the positions of individual nuclear spins in a single molecule

- **High spectral resolution**
  - → Routine in conventional ensemble NMR spectroscopy
  - → Measure nuclear species (^{1}H, ^{13}C, ^{19}F…)
  - → Measure *J*-couplings & chemical shifts with ppm accuracy

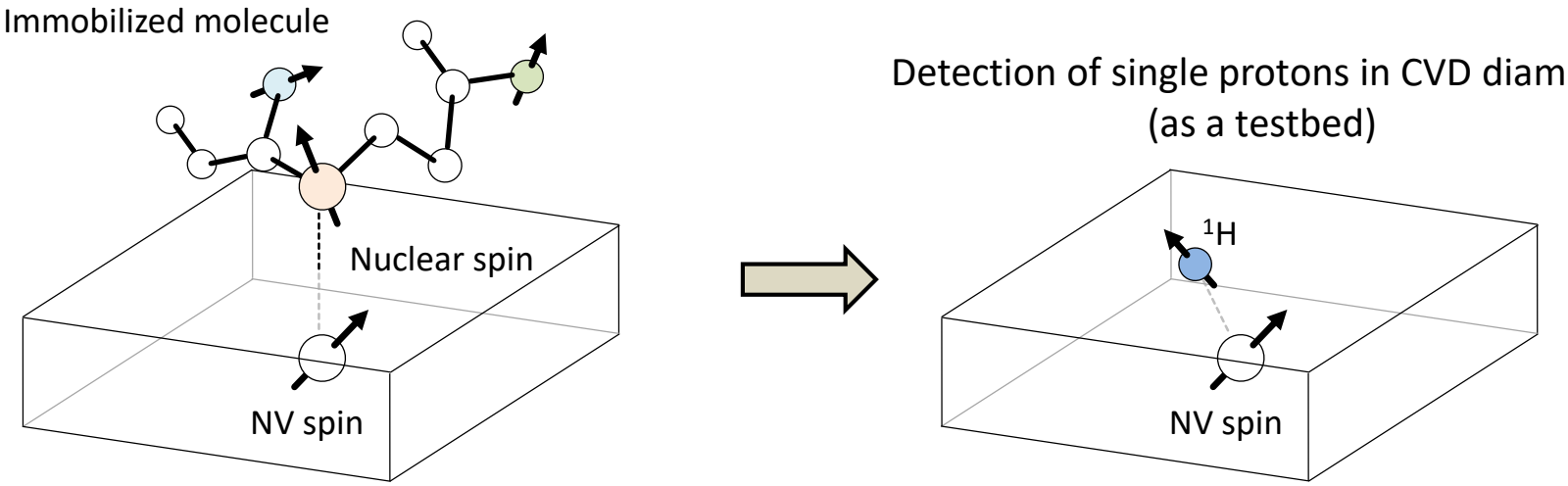

Sensing of single *n*-spin

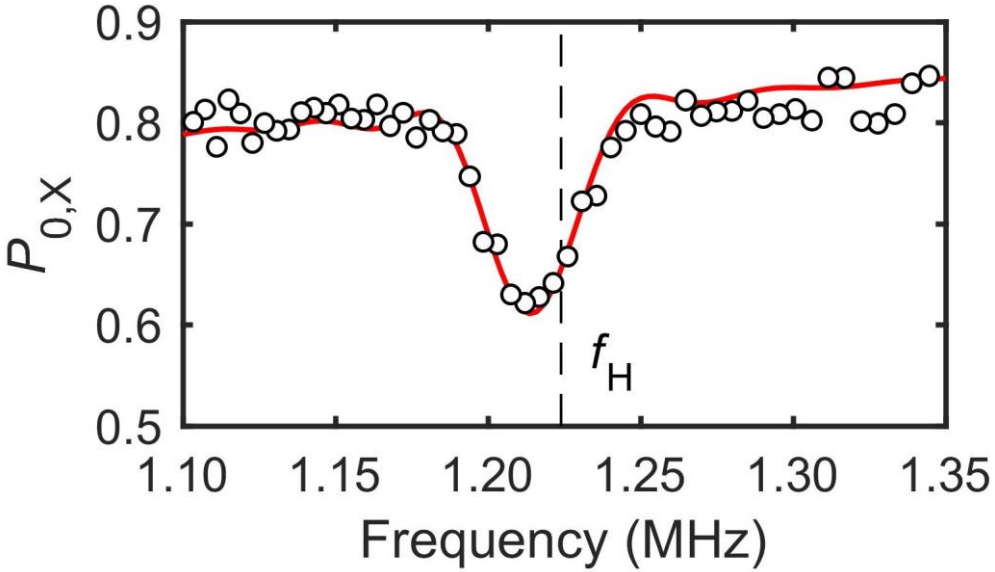

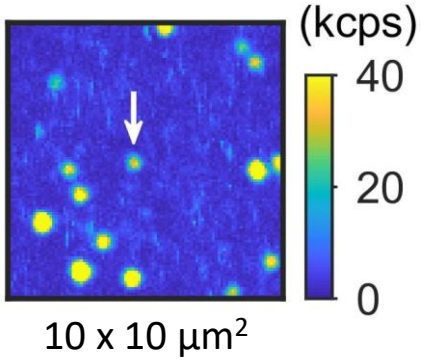

- Single NV in a N-doped CVD film ([^{12}C] = 99.999%)
- N = 64
- $f_H = \gamma_H B_0$ = 42.577 kHz/mT x 28.7 mT = 1.2239 MHz

Appl. Phys. Lett. **117**, 114002 (2020) Sasaki *et al.*

Correlation spectroscopy

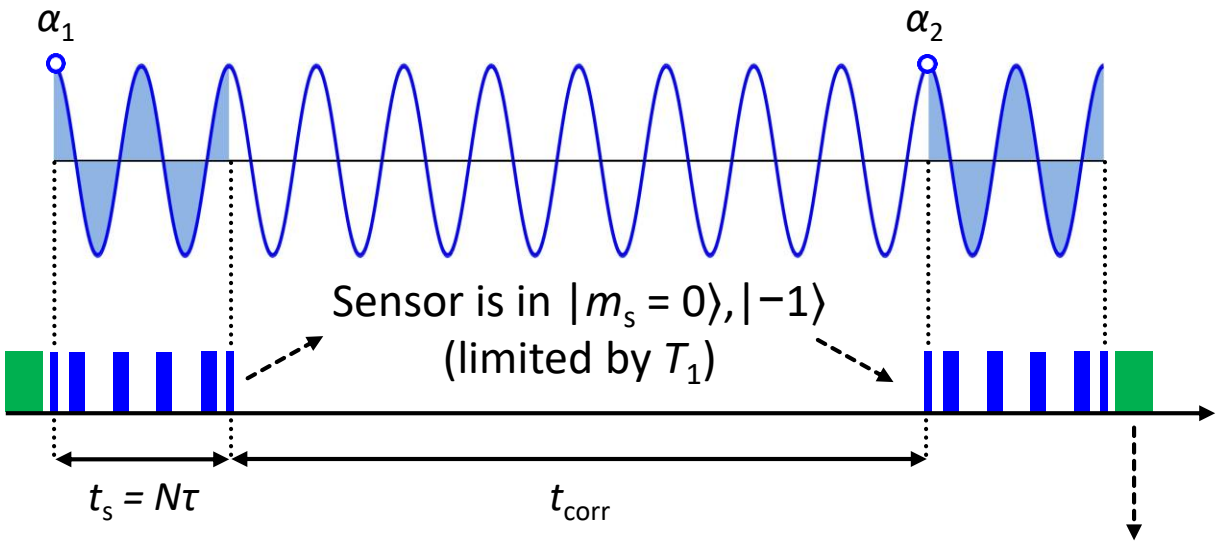

Accumulate more phase
if $t_{corr} = m/f_{ac}$

→ Sweep t_{corr}

The transition probability for random phases (α)

$$p(t_1) \approx \frac{1}{2}\left\{1 - \frac{1}{2}\left(\frac{\gamma B_{ac} t_s}{\pi}\right)^2 \cos(2\pi f_{ac} t_{corr})\right\}$$

Nature Commun. **4**, 1651 (2013) Laraoui *et al.*
Phys. Rev. Appl. **4**, 024004 (2015) Kong *et al.*
Nature Commun. **6**, 8527 (2015) Staudacher *et al.*
Phys. Rev. Lett. **116**, 197601 (2016) Boss *et al.*

Correlation spectroscopy of single *n*-spin

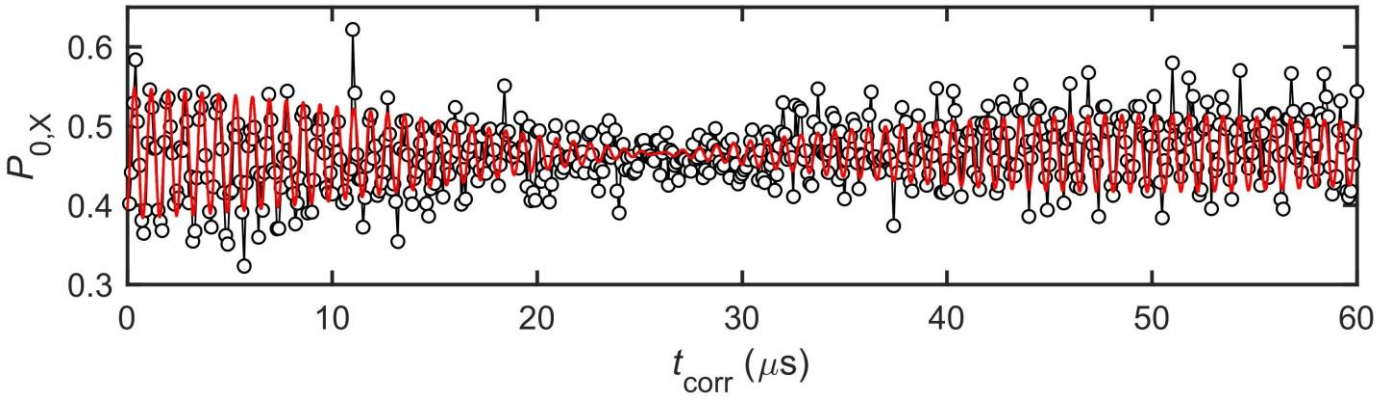

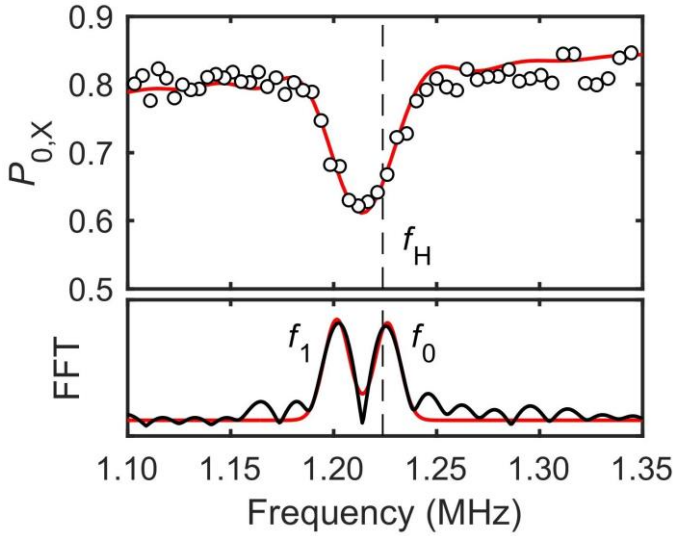

- f_0 = 1.2234 MHz
- f_1 = 1.2046 MHz

Appl. Phys. Lett. **117**, 114002 (2020) Sasaki *et al.*

Correlation spectroscopy of single *n*-spin

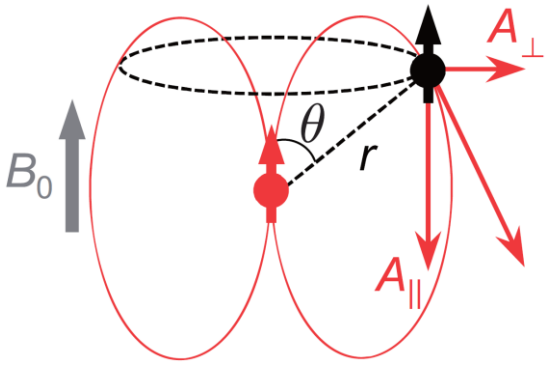

Hamiltonian of ^{1}H *n*-spin coupled with NV *e*-spin

$$H_{\mathrm{n}} = f_{\mathrm{H}} I_z + |m_s = -1\rangle\langle -1|(A_\parallel I_z + A_\perp I_x)$$

→ No hyperfine field when $|m_s = 0\rangle$

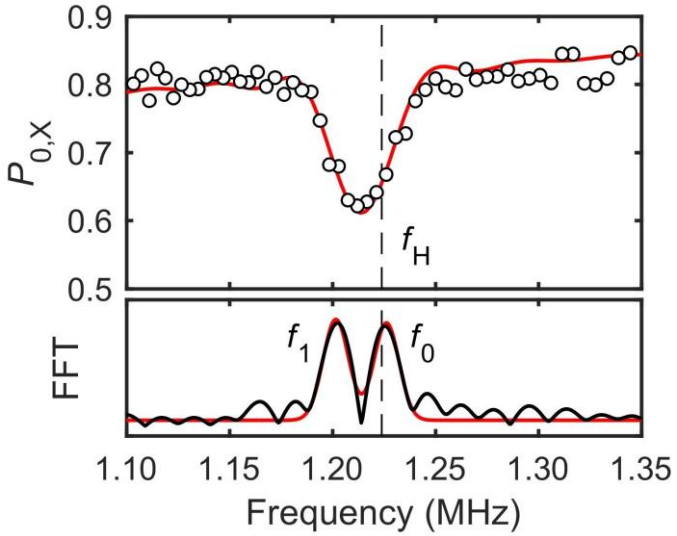

- f_0 = 1.2234 MHz = f_H (m_s = 0)
- f_1 = 1.2046 MHz = $f_H + A'_\parallel$ (m_s = −1)

$A'_\parallel$ = −18.8 kHz
$(f_0 + f_1)/2$ = 1.2140 MHz → dip

Appl. Phys. Lett. **117**, 114002 (2020) Sasaki *et al.*

Coherent control of single *n*-spin

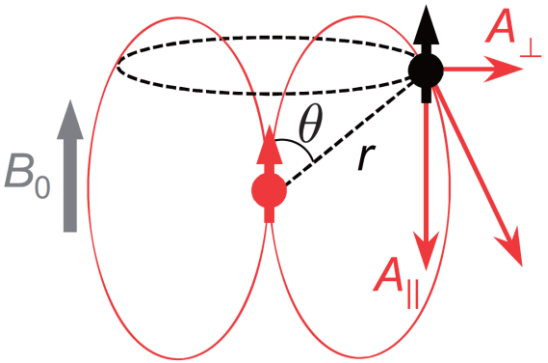

Hamiltonian of ^{1}H *n*-spin coupled with NV *e*-spin

$$H_{\mathrm{n}} = f_{\mathrm{H}} I_z + |m_s = -1\rangle\langle -1|(A_\parallel I_z + A_\perp I_x)$$

→ The single ^{1}H *n*-spin rotates about the $A_\perp$ axis

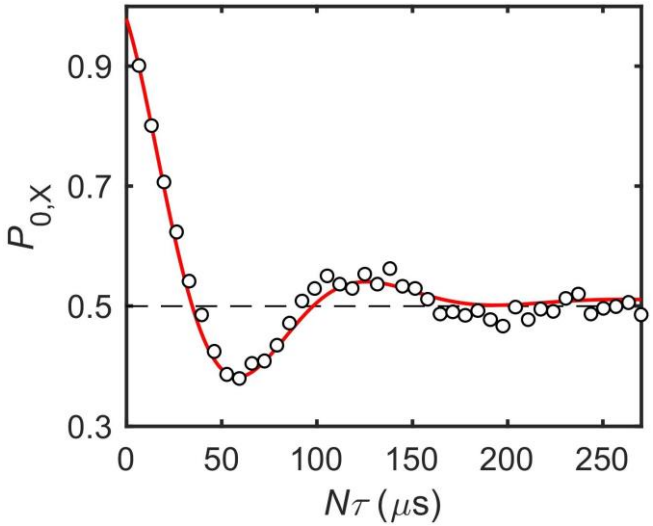

- $N \rightarrow 656$ (τ = 411.5 ns, fixed)
- f_{osc} = 7.414 kHz = $A'_\perp/2$

Appl. Phys. Lett. **117**, 114002 (2020) Sasaki *et al.*

Conditional rotation of single *n*-spin

e-spin control

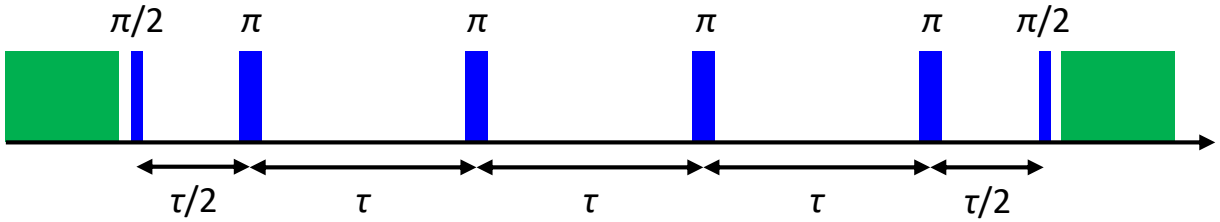

Evolution of *n*-spin vector

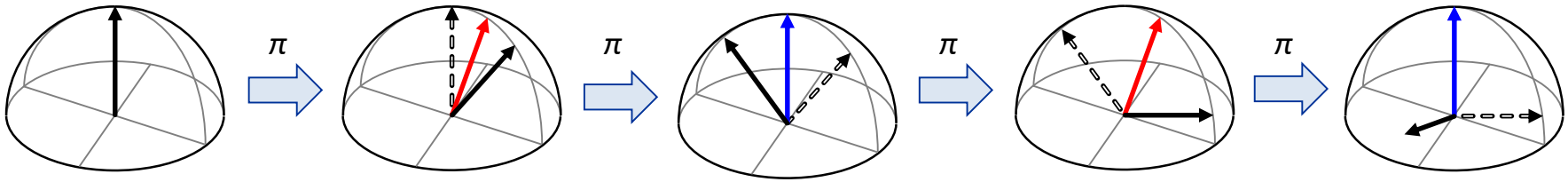

$t = 0 \rightarrow \tau/2$ $t = \tau/2 \rightarrow 3\tau/2$ $t = 3\tau/2 \rightarrow 5\tau/2$ $t = 5\tau/2 \rightarrow 7\tau/2$ $t = 7\tau/2 \rightarrow 4\tau$

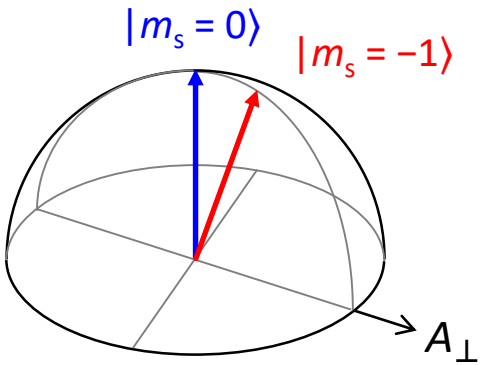

q-axis of *n*-spin

***Start from* $|m_s = 0\rangle$**

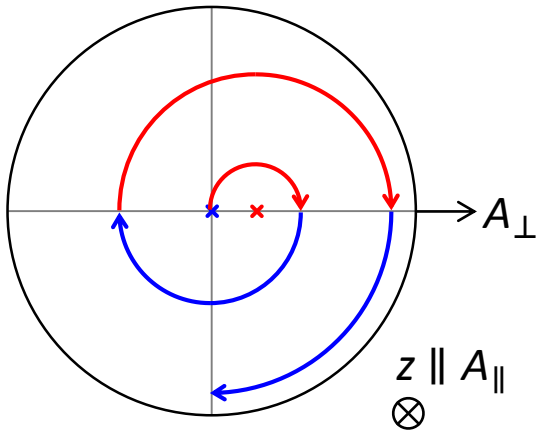

***Start from* $|m_s = -1\rangle$**

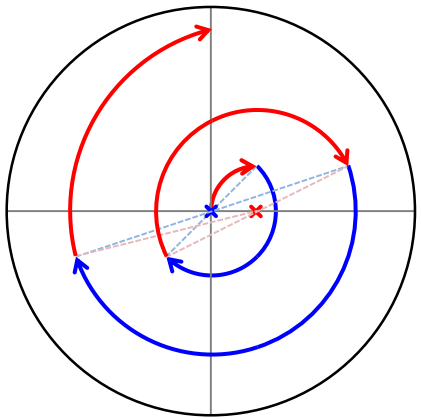

Coherent control of single *n*-spin

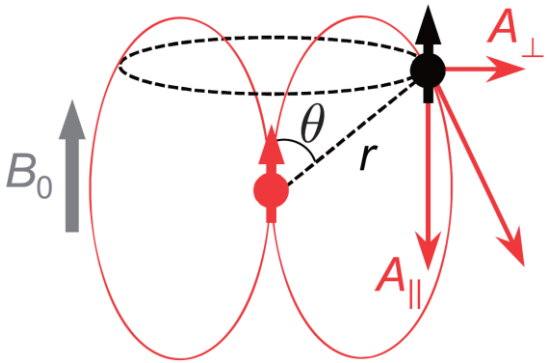

Transition probability of the NV spin

$$P_{0,\mathrm{X}} = 1 - \frac{1}{2}\left(1 - \underbrace{\boldsymbol{n}_0 \cdot \boldsymbol{n}_{-1}}_{-1}\right)\sin^2\frac{N\phi_{\mathrm{cp}}}{2}$$

Phys. Rev. Lett. **109**, 137602 (2012) Taminiau *et al.*

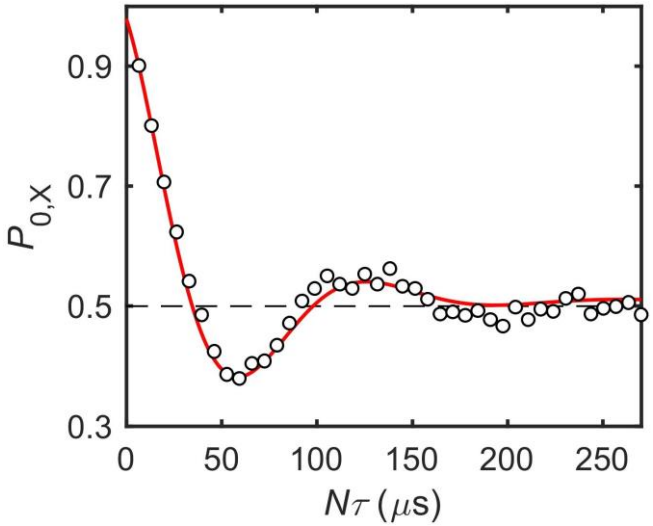

- $N \rightarrow 656$ (τ = 411.5 ns, fixed)
- f_{osc} = 7.414 kHz = $A'_\perp/2$

$P_{0,X} < 0.5$ (coherent rotation)
→ Single proton

Appl. Phys. Lett. **117**, 114002 (2020) Sasaki *et al.*

Determination of hyperfine constants

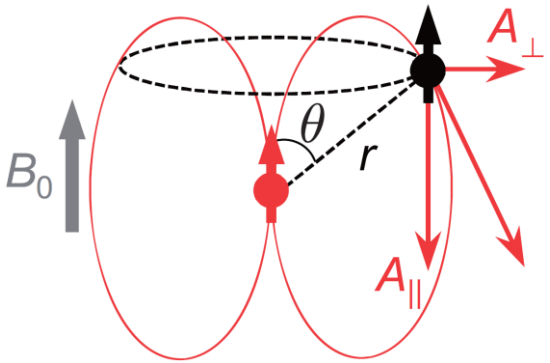

Magnetic dipole interaction

$$A_\parallel = h\gamma_e\gamma_H \frac{3\cos^2\theta - 1}{r^3}$$

$$A_\perp = h\gamma_e\gamma_H \frac{3\cos\theta\sin\theta}{r^3}$$

$A_\parallel$ = −19.0 kHz
$A_\perp$ = 22.9 kHz

⟺

r = 1.44 nm
θ = 72.3°

The position of the nucleus can be determined
→ Basis for single-molecular structure analysis

(Azimuthal angle ϕ can determined by RF control) Phys. Rev. B **98**, 121405 (2018) Sasaki *et al.*

Appl. Phys. Lett. **117**, 114002 (2020) Sasaki *et al.*

Magnetic field dependence

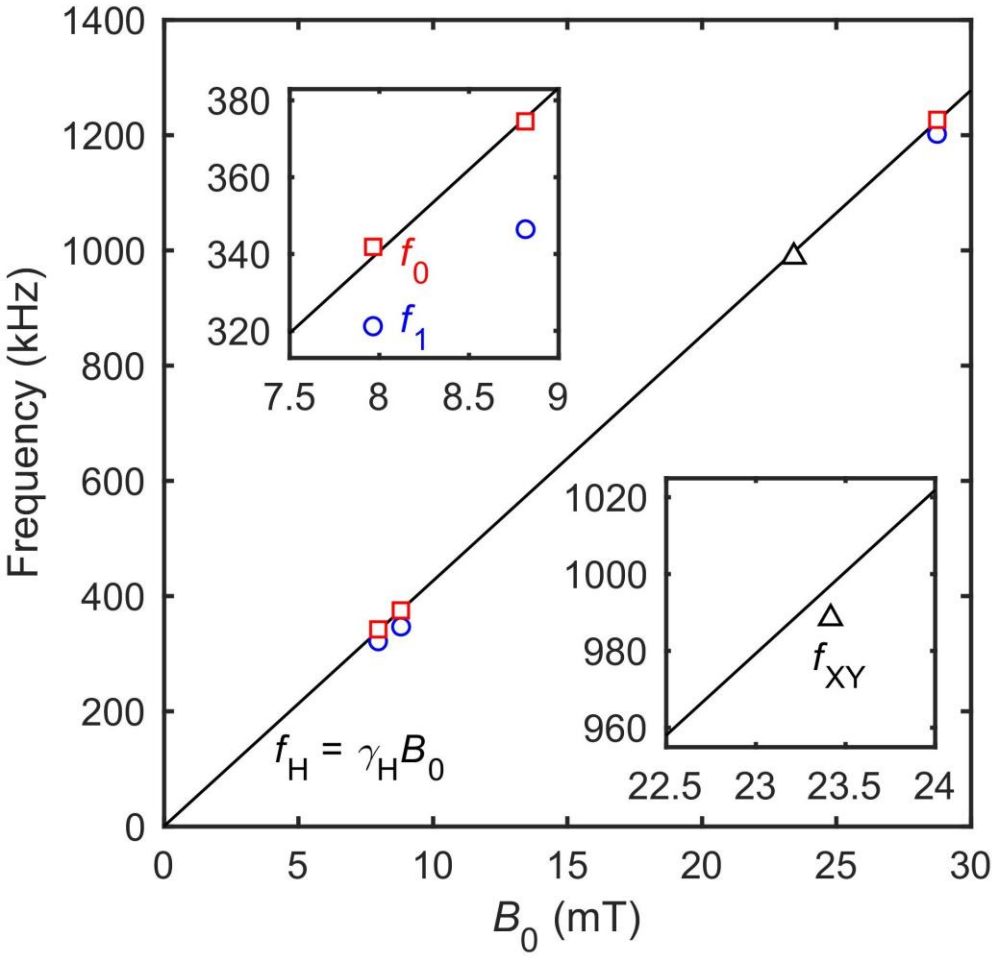

(γ_H/γ_C = 3.97 → Spurious harmonics?) Phys. Rev. X **5**, 021009 (2015) Loretz *et al.*

Appl. Phys. Lett. **117**, 114002 (2020) Sasaki *et al.*

Toward single-molecular imaging

- **High spatial resolution**
  - → Accurate measurement of *e*–*n* int. const's ($A_{\parallel}$, $A_{\perp}$) ≈ (r, θ)
  - → ϕ can be determined by RF control

- **High spectral resolution**
  - → Routine in conventional ensemble NMR spectroscopy
  - → Measure nuclear species (^{1}H, ^{13}C, ^{19}F…)
  - → Measure *J*-couplings & chemical shifts with ppm accuracy

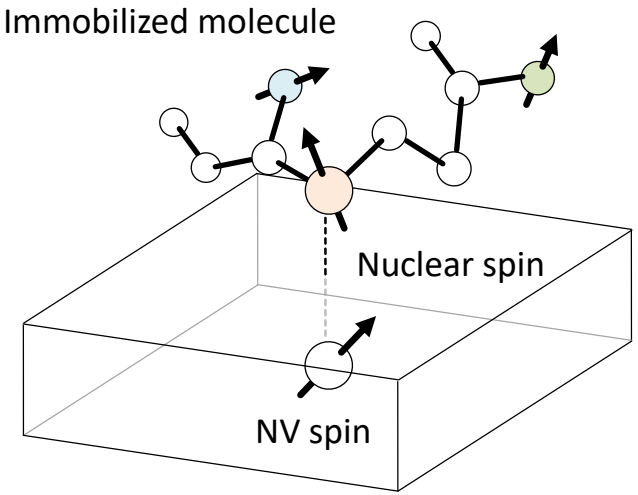

Not so easy with NV centers
Limited by sensor/memory spin lifetimes ($T_{2e/n}$, $T_{1e/n}$)

T_{2e} tends to be shorter for near-surface NV centers

AC magnetometry revisited

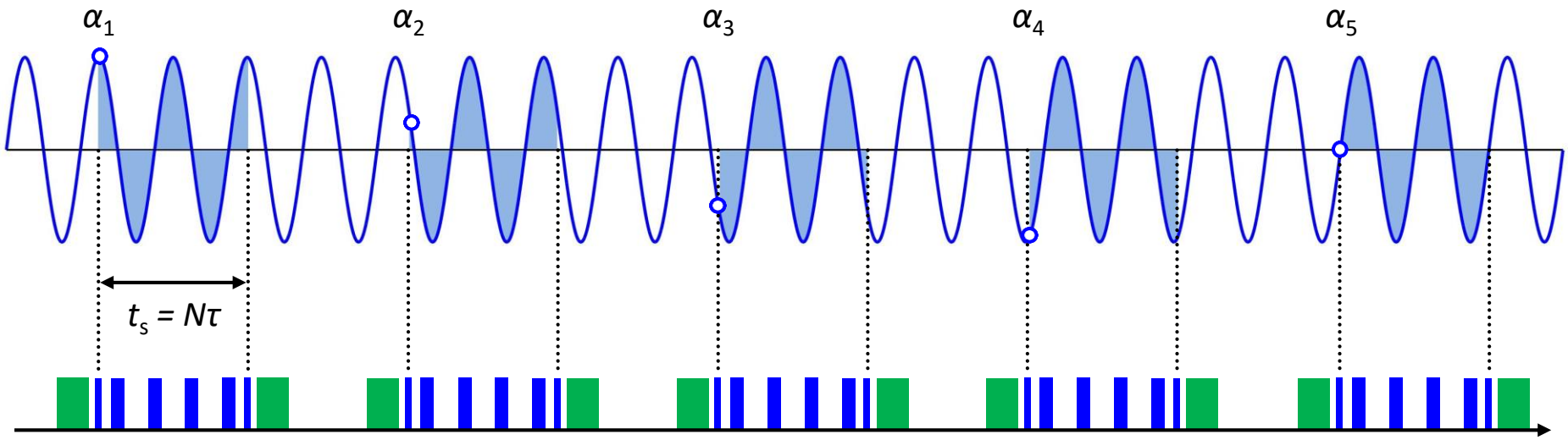

- $\varphi \propto \cos \alpha$
- Usually, we average over **random α**

AC magnetometry revisited

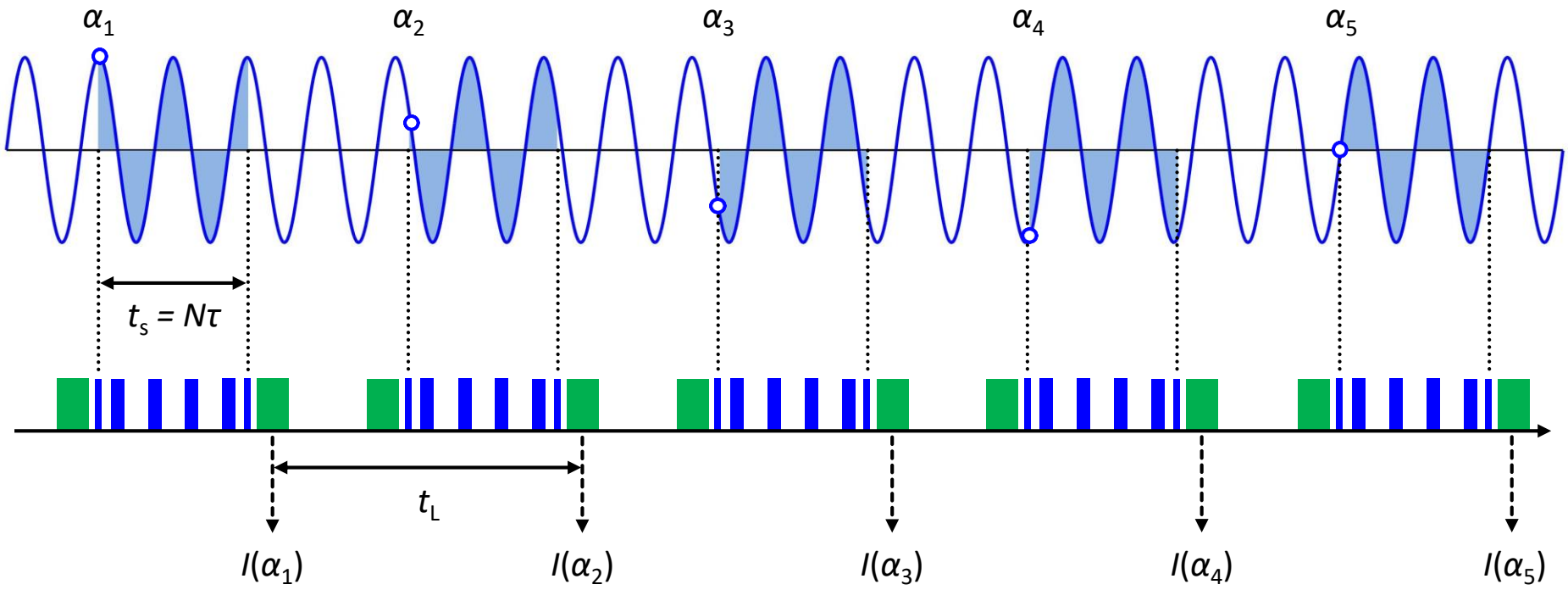

- $\varphi \propto \cos \alpha$
- Usually, we average over **random α**
- **If the data acq. is periodic,** adjacent α's are related by $\alpha_{k+1} = 2\pi f_{ac} t_L + \alpha_k$

Ultrahigh resolution sensing

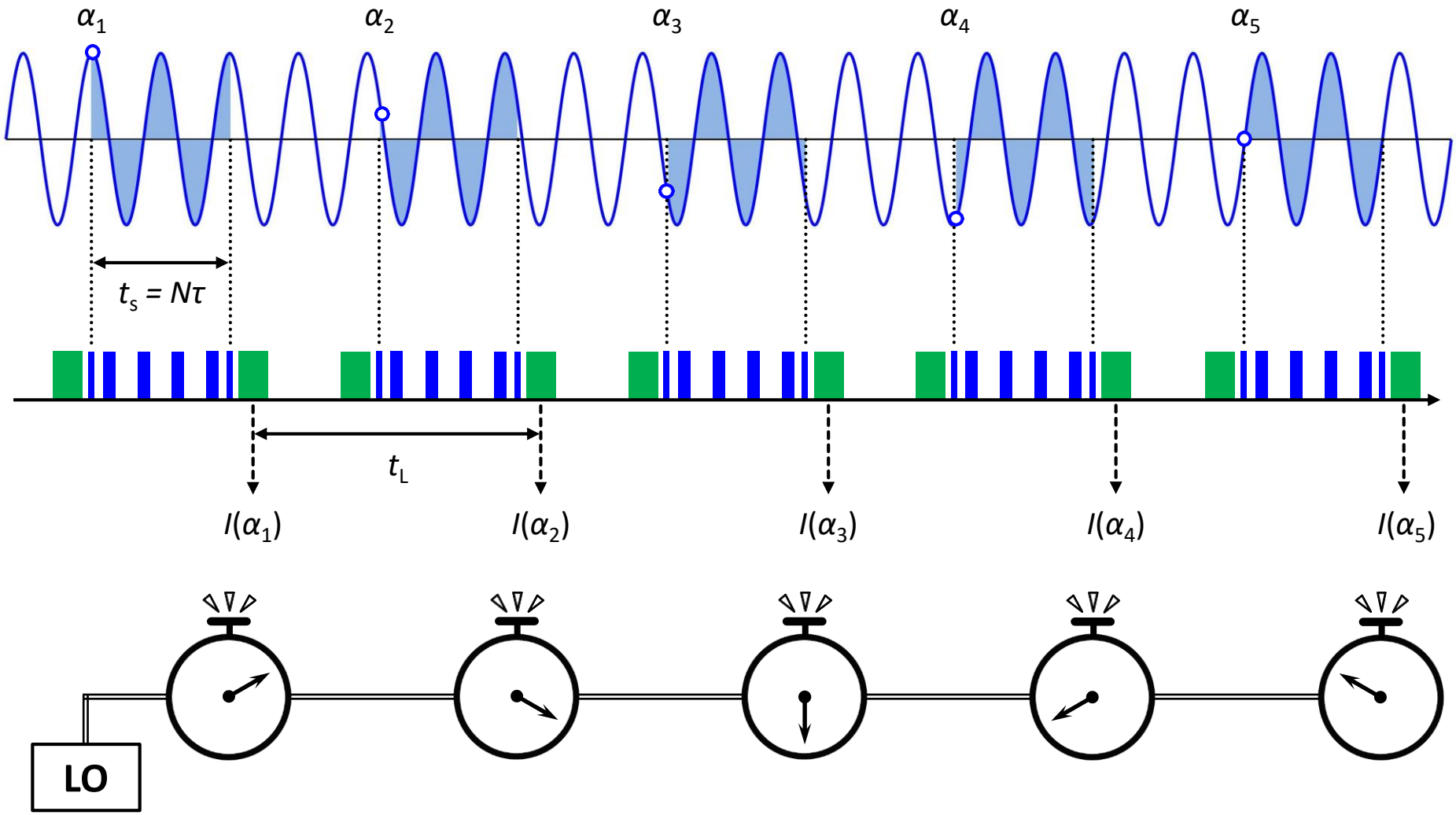

Undersampled, sensor-lifetime-unlimited signal

Science **356**, 832 (2017) Schmitt *et al.*; Science **356**, 837 (2017) Boss *et al.*; Nature **555**, 351 (2018) Glenn *et al.*

Ultrahigh resolution sensing

B_{ac} = 96.5 nT & f_{ac} = 2.001 MHz applied from a coil, detected by a single NV center

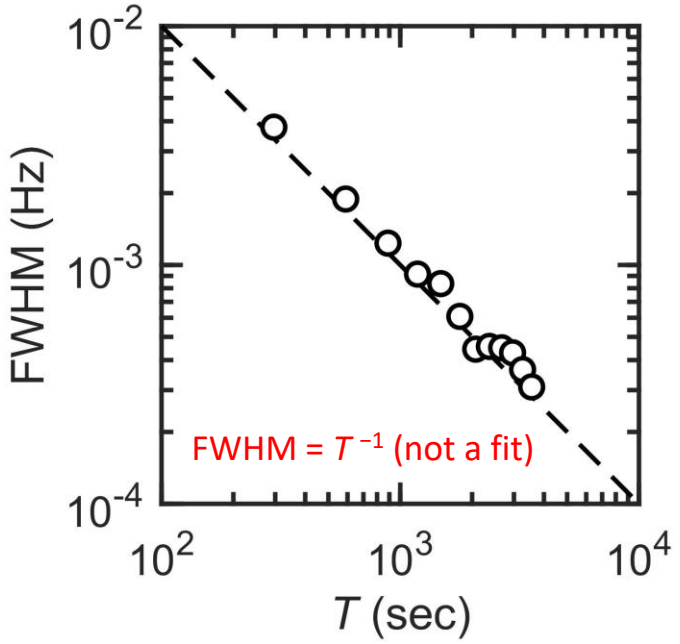

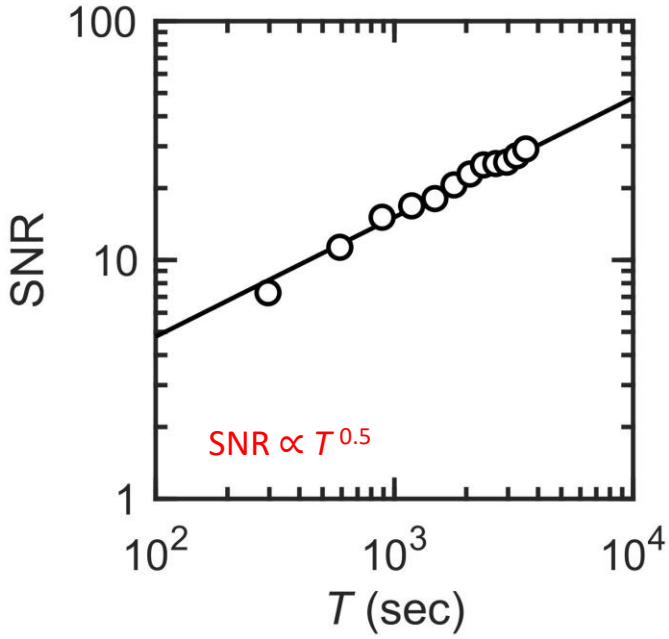

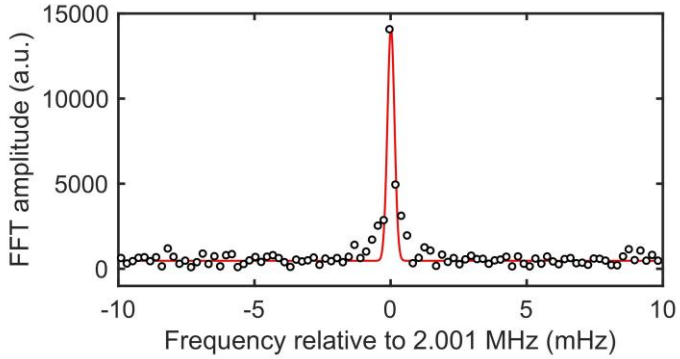

- T = 3600 sec
- FWHM = 0.304 mHz

J. Appl. Phys. **123**, 161101 (2018) Abe *et al.*

Free induction decay of single *n*-spin

RF control & free precession of *n*-spin

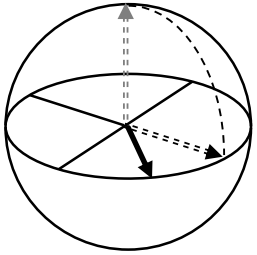

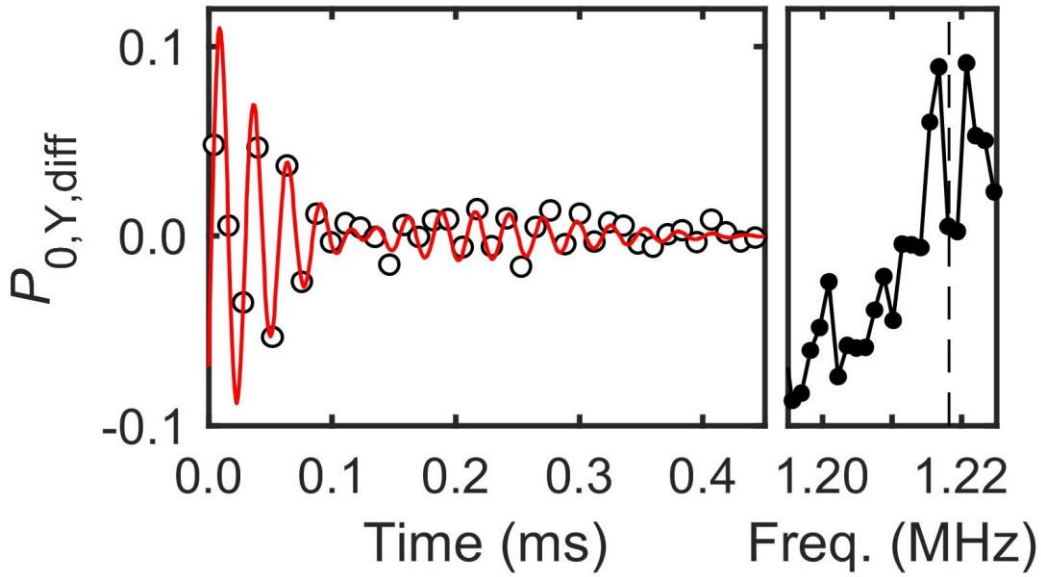

Nuclear Rabi oscillation

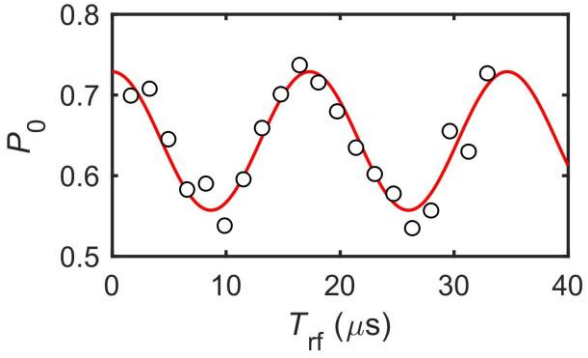

- $T_{rf,\,\pi/2}$ = 4.115 μs
- [PulsePol]–$T_{rf,\,\pi/2}$–[X/2–(XY16)–Y/2–L_{RO}]^{50}
- $f_{sample} = 1/t_L$ = 84.46 kHz
- $f_p = (f_0+f_1)(t_s/t_L)/2+f_0(t_s-t_L)/t_L$ = 1.2182 MHz
  → Split (analogous to chemical shifts)

Appl. Phys. Lett. **117**, 114002 (2020) Sasaki *et al.*

Summary

- **Tools for single-molecule imaging/structural analysis are being developed**
  - → Ultrahigh resolution sensing[1,2,3], resolving chemical shifts[3,4] & suppression of back action from *n*-spins[5,6]
  - → Determination of the positions of individual *n*-spins via RF control[7,8,9,10]
  - → Detection and control of single proton spins[11,12]
- **^{13}C *n*-spin cluster as a quantum simulator/computer**[13,14]

[1] Science **356**, 832 (2017) Schmitt *et al.* (Ulm)
[2] Science **356**, 837 (2017) Boss *et al.* (ETH)
[3] Nature **555**, 351 (2018) Glenn *et al.* (Harvard)
[4] Science **357**, 67 (2017) Aslam *et al.* (Stuttgart)
[5] Nature Commun. **10**, 594 (2019) Pfender *et al.* (Stuttgart)
[6] Nature **571**, 230 (2019) Cujia *et al.* (ETH)
[7] Phys. Rev. B **98**, 121405 (2018) Sasaki *et al.* (Keio)
[8] Phys. Rev. Lett. **121**, 170801 (2018) Zopes *et al.* (ETH)
[9] Nature **576**, 411 (2019) Abobeih *et al.* (Delft)
[10] Nature Commun. **13**, 1260 (2022) Cujia *et al.* (ETH)
[11] Phys. Rev. Lett. **113**, 197601 (2014) Sushkov *et al.* (Harvard)
[12] Appl. Phys. Lett. **117**, 114002 (2020) Sasaki *et al.* (Keio)
[13] Science **374**, 1474 (2021) Randall *et al.* (Delft)
[14] Nature **606**, 884 (2022) Abobeih *et al.* (Delft)